The Plug-in Hybrid Electric Refuse Vehicle Routing Problem for Waste Collection

Abstract

Commercial waste collection is an essential service requiring efficient and reliable provision for customers. At the operational level, one of the most challenging problems is to design a set of refuse vehicle routes to collect waste from a set of bins. To be used multiple times, these vehicles must be emptied regularly throughout the day. This paper investigates a waste collection problem with a homogeneous fleet of plug-in hybrid electric refuse vehicles powered by two different power sources, i.e., electricity and compressed natural gas (CNG). In addition, realistic fuel consumption functions are used to estimate total energy requirements for each type of fuel, including refueling and recharging, and the detailed energy consumption along the path between two nodes of interest. We propose a Hybrid Threshold Acceptance (HTA) algorithm for this problem and denote it as the Hybrid Waste Collection Problem (HWCP). Extensive computational experiments confirm that the proposed HTA algorithm provides good results against current state-of-the-art algorithms designed for the electric vehicle routing problem. Out detailed computational results demonstrate the performance of our method considering either full or partial recharging, as well as the effect of different battery/tank capacities. Compared to the standard CNG or electric vehicles, we also show the benefits of using a fleet of hybrid electric refuse vehicles in terms of operational costs and total distance traveled.

Keywords: Vehicle routing problem; Energy consumption; Plug-in hybrid electric vehicle; Metaheuristic algorithm

1. Introduction

Waste collection is one of the most challenging problems that could undermine governments' and local authorities' drive for sustainable development. Even a small improvement in waste management planning can yield significant opportunities for reducing total costs and improving public health (Eurostat, 2017; Mesjasz-Lech and Michelberger, 2019). The production of municipal solid waste is constantly increasing, with around 486 kg of domestic waste per capita generated in the European Union (EU) in 2017 (Eurostat, 2017). This paper investigates the waste collection problem from a logistical perspective.

This problem is known as the Waste Collection Vehicle Routing Problem with Time Windows (WCVRPTW), an NP-hard problem (Kim et al., 2006). The WCVRPTW extends the standard Vehicle Routing Problem with Time Windows by considering using intermediate facilities to empty the vehicles while collecting waste from households. In this problem, all locations (i.e., depot, customers' locations, landfill facilities) are known. Each location has a predefined time window during which a waste collecting refuse vehicle visit can take place. At the beginning of a service day, all refuse vehicles start from a central depot and visit customers to collect their waste. When a refuse vehicle is full, it must go to a landfill to empty its waste.

After unloading, the refuse vehicle returns to its duty. Given the increase in environmental interest in minimizing carbon dioxide-equivalent (CO_2e) emissions from transportation activities, the WCVRPTW has many real-life applications to optimize the routes and reduce man-made emissions. Practical waste collection studies have been conducted in Hong Kong (Lee et al., 2016), Vietnam (Louati, 2016), Denmark (Zbib and Wøhlk, 2019), and Portugal (Ramos et al., 2018).

As the literature shows, commercial, industrial, and residential waste are considered separately during their collection (Kim et al., 2006). In our research, we study the daily commercial waste collection problem. Day-to-day commercial waste represents a small share of the total waste produced. However, it has considerable potential in avoiding emissions due to the large geographical spread. These locations are often within the city center, where traffic and emissions are often regulated. Within the scope of this service, waste collection vehicles visit business customers (restaurants, shopping malls, retailers, and other commercial establishments). Each route may serve between 60 and 400 customers during which trips to landfills need to be arranged (Kim et al., 2006).

Real-life applications of the WCVRPTW may bring additional operational challenges, depending on the fleet's characteristics. This research incorporates several of such challenges, namely, *i*) a fleet consisting of plug-in hybrid electric waste collection vehicles; *ii*) the presence of recharging and fuel stations; and finally, *iii*) a realistic and microscopic fuel consumption function. In what follows, we explain these operational challenges in detail.

In most WCVRPTW studies, the collection of waste is performed using a fleet of vehicles operated with traditional internal combustion engines (ICEs) (see, e.g., Kim et al., 2006; Lee et al., 2016; Louati, 2016; Rabbani et al., 2018; Tirkolaee et al., 2019). However, this type of vehicle produces greenhouse gases (GHGs) (Demir et al., 2015). As an alternative, Electric Vehicles (EVs) (HVT, 2012) can be used by waste collection companies, and some models are available in different markets.

Due to current technological limitations on EVs, hybrid vehicles offer a more reliable option than pure EVs. These vehicles have a battery, an ICE, and an electric machine (EM). Using this technology, Plug-in Hybrid Electric Vehicles (PHEVs) link both EM and ICE to the wheels, and a vehicle can be operated on ICE or EM. In general, PHEVs run on battery power as a primary fuel source; when it is depleted, the vehicle runs on petrol, which again leads to emissions (Murakami, 2018). Hence, PHEV fleets should be utilized by incorporating alternative fuels, such as biodiesel, natural gas, or compressed natural gas (CNG) (US DOE, 2011). CNG can be used as an alternative fuel with a conventional diesel internal combustion engine where the engine regulates the natural gas pressure (Chen et al., 2018).

With this motivation, we consider the WCVRPTW with a fleet of PHEVs powered by two types of fuel: electricity and CNG (CNG-PHEV). We investigate PHEVs considering real applications, such as the private waste and recycling company Renova AB in Sweden. The company is managed by 11 local authorities and provides local councils and businesses with a fleet of CNG and CNG-PHEVs for waste collection (Renova, 2006). Other CNG-PHEV applications in operation are Green Fleet (2008) and Advantage Environment (2011).

Thus, the main motivation of this research is to introduce a new variant of the WCVRP that contains new technological advancements, such as using CNG-PHEV, which appear in reality and are used effectively in the field of waste collection.

From the WCVRPTW point of view, including a CNG-PHEV fleet and realistic consumption modeling changes the problem in three ways:

i) Two types of recharging stations must be considered, CNG and electricity, since the classical WCVRPTW does not consider refueling stations (not even traditional petrol stations).

ii) With hybrid vehicles, driving range limitations must be considered. Therefore, these vehicles need to be charged en route. There is a rich literature on the driving range of hybrid vehicles and the necessity for refueling at specialized stations (e.g., Arslan et al., 2015; Mancini 2017; Yu et al., 2017). The standard objective in these studies is to plan routes efficiently while considering both customers' visits and visits to stations. In our case, we consider visiting recharging and refilling stations while collecting waste from customers and disposing of this waste at specialized facilities.

iii) The use of an alternative fuel in routing problems is usually studied under GVRPs (Erdoğan and Miller-Hooks, 2012). However, most of these studies consider the energy consumed as a linear function of the distance (e.g., Nejad et al., 2017; Mancini 2017; Yu et al., 2017). This assumption is not practical since fuel consumption depends on many factors, such as speed, fuel type, vehicle load, road slope, etc. (Bektaş and Laporte, 2011). We adopt the CMEM of Barth and Boriboonsomsin (2009) to estimate fuel consumption.

To sum up, our problem considers CNG and PHEVs to solve the WCVRPTW. We call this problem the Hybrid Waste Collection Problem (HWCP). The HWCP can be seen as a combination of the classical WCVRPTW, which is NP-hard (Kim et al., 2006), and the HVRP, which is also NP-hard (Yu et al., 2017). The WCVRPTW is naturally NP-hard, and it is extremely difficult to obtain optimal solutions using standard mathematical solvers. Few used mathematical programming solvers (Tirkolaee et al., 2019) and most developed various approximation algorithms to solve the WCVRPTW and related extensions (Kim et al., 2006; Hannan et al., 2017; Liu and He, 2012). Regarding the HVRP, exact methods can only solve small-sized instances within reasonable computation times. Like in the WCVRPTW, most recent state-of-the-art algorithms developed for the HVRP can only solve small-sized instances (e.g., Mancini, 2017; Yu et al., 2017). Due to these difficulties, we propose a Hybrid Threshold Acceptance (HTA) metaheuristic algorithm to solve the HWCP.

One challenge in most realistic applications of routing CNG plug-in hybrid electric refuse vehicles is that this technology poses new and challenging operational problems related to logistics distribution. For example, plug-in hybrid vehicles have limited battery/CNG capacities, leading to a relatively short driving range compared to ICE vehicles. The scarcity of CNG stations needed to refuel these vehicles and the fact that they are usually not evenly distributed, unlike the widely available gas stations (Shao et al., 2020), increase the complexity of finding an efficient solution. The challenge of this proposed problem is to efficiently plan routes while considering both customers' visits and frequent visits to recharging and refueling stations during the working day.

From an industrial perspective, considering new types of vehicles creates difficulties for planning their routes and assigning customer locations to these different vehicles. This eventually requires more advanced

and capable solution algorithms. Our research contributes to both the agenda of industry and academia as we provide algorithmic solutions to handle all reflected issues.

The main contributions of our paper are threefold. First, we explore an extension of the WCVRPTW problem with a CNG-PHEV fleet and intermediate facilities for recharging and refueling, and test it on the traditional waste collection vehicle routing problem. In addition, our model considers a detailed and realistic fuel consumption function. Second, we propose an HTA metaheuristic algorithm for the HWCP. We develop several diversification and intensification mechanisms embedded into a new TA framework, leading to improved performance of our HTA algorithm. These include a crossover operator, a multi-start approach, and a shaking phase of variable neighborhood search for a better intensification. Finally, the results of extensive computational experiments show that our algorithm provides competitive results against the state-of-the-art ones by testing our method on a special case of the HVRP from the literature. We show the benefits of using a fleet of CNG-PHEV compared to pure electric and CNG vehicles in terms of travel distances and costs. Moreover, we also show that our different intensification and diversification mechanisms are required to improve the convergence of the traditional TA.

The remainder of this paper is organized as follows: Section 2 provides an overview of the recent literature related to our problem; Section 3 gives a formal definition, while Section 4 provides a mathematical model for the proposed problem. Section 5 describes our proposed HTA algorithm; Section 6 reports the computational results obtained with HTA; and finally, Section 7 provides conclusions and discusses the future research directions.

2. Literature review

This section summarizes the recent waste collection and green/hybrid VRP studies in the literature. First, metaheuristic approaches and concepts studied in the WCVRPTW are provided. Then, we look at the most recent research studies on green/hybrid VRPs. Finally, we also briefly review the relevant literature on measuring fuel consumption in VRPs.

2.1. The waste collection vehicle routing problems

The WCVRPTW was first formalized by Kim et al. (2006). The authors investigated the commercial problem with multiple trips and a lunch break for drivers, and proposed an extension of the insertion algorithm of Solomon (1987) for solving the problem. In the study of Benjamin and Beasley (2010), the WCVRPTW with a homogeneous fleet of vehicles, landfill facilities, and driver rest periods is considered. The authors proposed a VNS algorithm to solve this variant of the WCVRPTW. The proposed algorithm is tested on newly generated instances containing 19 landfill facilities and around 2,000 customers on the WCVRP with lunch break instances of Kim et al. (2006). Recently, Tirkolaee et al. (2019) developed an SA algorithm to solve a WCVRP with multiple trips.

Due to the complexity of the WCVRPTW and its variants, the problem cannot be solved effectively using state-of-art solvers within reasonable computational times (Wei et al., 2019). Therefore, several metaheuristics algorithms were developed in the literature. These include Variable Neighborhood Search (VNS) (Polacek et al., 2007); Ant Colony Optimization (ACO) (Bautista et al., 2008; Liu and He., 2012); Genetic Algorithm

(GA) (Karadimas et al., 2007); Simulated Annealing (SA) (Tirkolaee et al., 2019); and Particle Swarm Optimization (PSO) (Hannan et al., 2017).

Different sets of realistic constraints in the WCRPTW can be found in Hannan et al.(2017), Nowakowski et al.(2018), and Zbib and Wøhlk (2019). For more details on the WCVRPTWs, interested readers are referred to the studies of Han and Cueto (2015) and Sulemana et al. (2018).

2.2. The hybrid vehicle routing problems

Under the green VRP (GVRP) literature, the hybrid version (HVRP) extends the purely electric VRP (EVRP). The main difference is that the PHEV fleet uses two different fuels (e.g., electricity and diesel/gasoline), while in the EVRP, only electricity is used.

In recent years, the EVRP has received attention from researchers due to the benefits of EVs to the environment. Tahami et al. (2020) studied the Capacitated VRP using a fleet of EVs. To solve this problem, the authors developed a branch-and-cut (B&C) and a hybrid method. The methods were tested on newly generated instances based on the EVRP benchmark instances of Schneider et al. (2014). In another problem, Lin and Kuo (2021) investigated the benefits and deployment of EVs in the carsharing problem by considering stochastic demand and parking space to maximize the total expected profit. Wang et al. (2021) developed an exact method based on B&C to solve the electric location routing problem by considering multiple types of chargers for EVs. Lu et al. (2022) studied a fleet composed of electric and gasoline taxis to jointly serve a set of passengers and parcels by using recharging stations. A matheuristic is developed and tested on real-world instances from a taxi company in Kaohsiung, Taiwan. Recently, Basso et al. (2022) studied the dynamic stochastic EVRP. A Reinforcement Learning approach is developed and tested in real-life instances from Luxembourg. EVs are an emerging trend in VRP variants but not yet in the WCVRP. Interesting survey papers on the application of EVs are those of Bektaş et al. (2019), Kucukoglu et al. (2021), and Abid and Tabaa (2022).

The HVRP with PHEVs has not been widely studied. In one of the earliest studies, Nejad et al. (2017) developed exact methods and an approximation procedure to solve a real-life routing problem in Southeast Michigan, US. Later, Mancini (2017) provided an integrated MILP model with a distance-based constant fuel consumption rate. The author developed a Large Neighborhood Search (LNS) algorithm to solve the GVRP using the benchmark instances of Erdoğan and Miller-Hooks (2012). The results showed that the LNS algorithm provides better solutions than the state-of-the-art algorithms for the GVRP. Like Mancini (2017), Vincent et al. (2017) developed two versions of a SA algorithm using the Boltzmann and Cauchy functions. The proposed methods were tested on the capacitated VRP benchmark instances. Hiermann et al. (2019) developed a new HVRP variant by considering different vehicle types (electric vehicles, PHEVs, and ICEVs) and recharging stations. A hybrid GA was used on EVRP benchmark instances. Recently, Bahrami et al. (2020) studied the HVRP by considering the powertrain control of the PHEV. The authors developed a branch-and-cut (B&C) and a heuristic algorithm to solve a real-life case in Toronto, Canada.

In most HVRPs, only the recharging of the electric battery of the PHEVs is considered. The surveys of Pelletier et al. (2017) and Asghari et al. (2020) provide more details on both EVRPs and HVRPs with various types of electric vehicles. Our research considers visiting recharging and refueling stations while collecting

waste. Considering two sets of fuel stations in the planning phase is more complex than assuming a single type of fuel station (Yu et al., 2017).

2.3. Measuring fuel consumption in routing problems

In addition to the routing problem, we further investigate energy consumption by adopting the Comprehensive Modal Emissions Model (CMEM) for hybrid refuse vehicles.

The energy consumption depends on several attributes, such as acceleration/deceleration, speed, and road gradient. Most EVRP studies considered these main factors affecting fuel consumption (e.g., Travesset-Baro et al., 2015; Montoya et al., 2016; Koç et al., 2019). Macrina et al. (2019) studied vehicle speed, acceleration, and deceleration in urban areas. In their study, the CMEM considers three phases h (h = 1, 2, 3) for each arc (i, j): an acceleration phase (h=1), a deceleration phase (h=3), and a constant speed value is considered as the second phase (h=2), resulting in a trapezoidal function ($1 \rightarrow 2 \rightarrow 3$) or triangular function ($1 \rightarrow 3$). In many other studies, including the one proposed by Macrina et al. (2019), the effect of road gradient on fuel consumption is also neglected and assumed to be zero in all arcs. However, it is known that the road gradient has one of the most significant influences on vehicle fuel consumption, as shown in Masmoudi et al. (2018b). Heni et al. (2019) developed the traditional CMEM by considering both fixed speeds or different speeds over time for each arc. Recently, Heni et al. (2021) provided effective machine learning tools to estimate fuel consumption by considering more realistic conditions than traditional CMEM, such as the time-varying speed and traffic frequency. Following this recent literature, we consider all the main factors, including vehicle speed, acceleration, deceleration, road gradient, environment, and traffic-related factors, as discussed in Demir et al. (2014).

3. Problem description

The goal of HWCP is to determine a set of CNG-PHEV routes to empty waste bins at a minimum cost. A solution to the HWCP must satisfy the following conditions:

- All waste bins must be emptied.
- A customer is visited by only one vehicle.
- The total waste from the visited bins must not exceed the vehicle capacity, such that if it is full, then the vehicle should go to the landfill facility to be emptied before servicing the next customer.
- Each vehicle can make multiple landfill visits during its working day.
- Each customer should be served within its time windows, such that if a vehicle arrives early, it must wait until the beginning of the time window.
- Each recharging/refueling *station* can be visited multiple times.
- Each vehicle can visit a station node when the remaining power type level in its battery and tank is not sufficient to visit the next customer. We note that the CNG fuel is used only if the energy of the vehicle is not enough to visit the next node.
- Each time a vehicle visits a station, the corresponding fuel is refilled until it reaches the maximum capacity.
- Each vehicle must return empty to the depot.

• And finally, each route should start and end at the depot while satisfying the maximum working time.

3.1. Modeling CNG fuel consumption for the PHEVs

In the standard VRP, all vertices can be visited by any vehicle, and each edge directly links a vertex to another. In a real-world network, there is not one edge directly linking each pair of vertices; there are many intersections in what is, in fact, a path between two locations (Jaballah et al., 2021). Moreover, while in the VRP one minimizes the total distance or time, when using a comprehensive consumption function, many other factors are considered, such as the slope of the segments being traversed (Demir et al., 2011; Heni et al., 2019). The cost-minimizing path might then not be the shortest one.

In most of the literature, each arc (i, j) connecting nodes i to j is assumed to be a direct link and ignores the underlying street network. In other words, these studies only consider a reduced graph by using visited nodes i and j, without considering the intersections within each path (i, j). We consider a more realistic network by also including intersections. In a real-world shortest path problem (SPP), each vertex denotes an intersection, and each edge denotes a road segment between intersections (Murakami, 2017; 2018). For example, each arc (i, j) represents segments in which intersection nodes are associated with the arc (Fig.1.a). For example, in Fig (1.b), to travel from node i to node j, a refuse vehicle must pass through two intersections, A and B, which form three segments. Thus, in our model, we incorporate several intersection points between each arc (i, j) by using different road gradient values on each segment forming an arc (i, j). Let S_{ij} be the set of segments of arc (i, j), indexed by s. The relevance of using such a modeling approach is to allow the vehicle to change driving modes (fuel, battery, CNG) for each traversed segment.
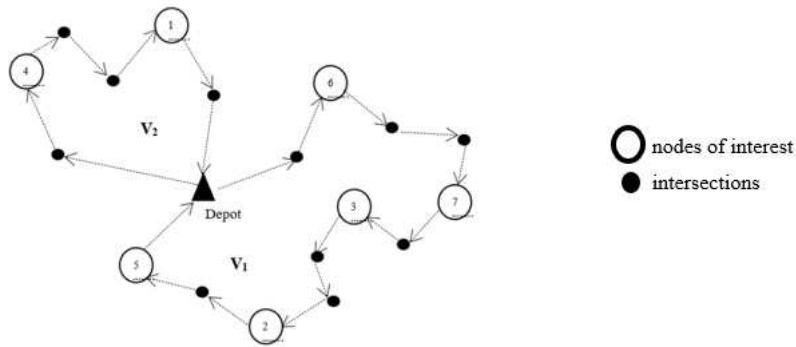

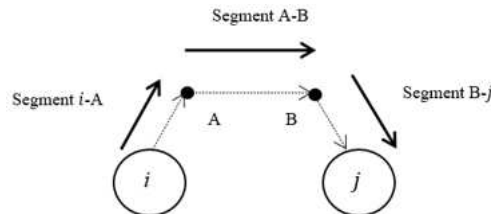**Fig. 1.a**. An example of segments forming the edges

Fig. 1.b. Three segments forming arc (i, j)

Figure 1. Modeling the road network with intersection nodes

In this research, the CNG-PHEVs are powered by two fuel source types, e and r, which refer to the electricity and the CNG, respectively. Thus, it is necessary to develop a consumption fuel rate for each fuel

type throughout each segment s of arc (i, j). We discuss the energy consumption function based on Macrina et al. (2019).

We adopt the traditional mechanical power developed by Bektaş and Laporte (2011) to define the mechanical power of each segment s of arc (i, j), as denoted by p_s^M that can be expressed by function (1):

$$p_s^M [\text{kW}] = (g\sin(\alpha_{ij_s}) + gC_r\cos(\alpha_{ij_s})(Q_i + w)) + (0.5C_d A\rho)v_s^2)v_s, \qquad (1)$$

where g is a constant parameter representing the gravitational constant, C_r and C_d represent rolling resistance and aerodynamic drag coefficients, and α_{ij_s} is the gradient of the road of segment s in arc (i, j). Let w be the curb weight of a vehicle, and Q_i be the quantity of waste in the vehicle after visiting customer i; the frontal surface area of the refuse vehicle is denoted by A; ρ is the air mass density; and v_s is the vehicle speed traversing segment s. Hence, the energy consumption p_s^E for segment s of arc (i, j) of distance d_s can be defined as described in function (2):

$$p_s^E(Q_i)[\text{kW}] = (p_s^M(Q_i)/\eta)\, d_s, \qquad (2)$$

where η represents energy efficiency from battery-to-wheel, defined by inequality (3), in which η takes a positive value η^+ when operating as a motor to discharge electric energy and a negative value η^- when acting as a generator to recover energy during the regenerative state.

$$\eta = \begin{cases} \eta^+ \leq 1, & \text{if } p_s^E(Q_i) > 0 \text{, and } 0 \leq p_s^M(Q_i) \leq 100\ kW \\ \eta^- \geq 1, & \text{if } p_s^E(Q_i) < 0 \text{, and} -100 \leq p_s^M(Q_i) \leq 0\ kW. \end{cases} \qquad (3)$$

Thus, based on equations (1) and (2), and following the CMEM as in Macrina et al. (2019), the energy consumption for the electric power type e of the vehicle for a segment s of arc (i, j) can be calculated with function (4):

$$p_{ij_s}^e(Q_i)\,[\text{KW}] = \sum_{h=1,2,3}([(a(d_{ij_{sh}}) + g\sin(\alpha_{ij_s}) + gC_r\cos(\alpha_{ij_s})(Q_i + w) + (0.5C_d A\rho)v(d_{ij_{sh}})^2]v\,d_{ij_{sh}}/\eta)\,\overline{d_{ij_{sh}}} \qquad (4)$$

where $a(d_{ij_{sh}})$ represents both acceleration and deceleration phases h, where $d_{ij_{sh}}$ is the distance of segment s in arc (i, j); and $v(d_{ij_{sh}})$ represents vehicle speed at the beginning of state h traversing a segment s in arc (i, j).

Thus, the energy rate p_{ij}^e for each arc (i, j) can be calculated as defined in function (5):

$$p_{ij}^e(Q_i)[\text{kW}] = \sum_{s \in S_{ij}} \sum_{h=1,2,3} p_{ij_{sh}}^e(Q_i). \qquad (5)$$

The contribution of existing studies with the consideration of CNG fuel (Zhang et al., 2014; Xu et al., 2015; Ercan et al., 2015) is to utilize the MOVES (MOtor Vehicle Emission Simulator) function proposed by the EPA (EPA, 2012). One of the disadvantages of this model is that it requires several input profiles (Wang and Rakha, 2018), which is time-consuming. As a more practical and potentially effective approach, we apply CMEM to estimate the CNG fuel consumption for CNG-PHEV.

The fuel consumption for the CNG power type r of the vehicle for arc (i, j) can be calculated as:

$$FR_{ij}^r(Q_i) = \sum_{s \in S_{ij}} \sum_{h=1,2,3} max\left\{\frac{\xi}{\tau\vartheta}\left(f\text{ND} + \frac{M_{ij_{sh}}}{\mu.\mu_t}\right), 0\right\}, \qquad (6)$$

where ξ is the fuel-to-air mass ratio, τ is the heating value of a typical CNG fuel, ϑ is a factor converting the fuel rate from gram-per second to litter-per second, f is the engine friction factor, N is the engine speed, D is

the engine displacement parameter, μ is the efficiency parameter for CNG engines, μ_t is the drive train efficiency parameter, and $M_{ij_{sh}}$ represents the mechanical power as defined by Macrina et al. (2019):

$$M_{ij_{sh}} = [(a(d_{ij_{sh}}) + g\sin(\alpha_{ij_s}) + gC_r\cos(\alpha_{ij_s})(Q_i + w) + (0.5C_dA\rho)v(d_{ij_{sh}})^2]v(\overline{d_{sh}}). \qquad (7)$$

Physical constants and other parameters for the CNG-PHEVs are adopted from Macrina et al. (2019). These notations are also provided in Appendix A.

4. Model formulation

In the HWCP, let $B = \{1,\dots,b\}$ the set of b customers and $L = \{1,\dots,l\}$ the set of l landfills. In addition, let F_z be the set of z alternative fuel stations. The set F_z is also divided into two type station subsets $F_z = F_e \cup F_r$, where $F_e = \{1,\dots,e\}$ is the set of e charging stations, and $F_r = \{1,\dots,r\}$ is the set of r refueling stations. In addition, copies of the recharging and refueling stations allow multiple visits to the same station. Thus, F_z' is the set of dummy vertices to allow multiple visits to each node in the set F_z of stations, where $F_e' = \{e+1,\dots,e+e'\}$ and $F_r' = \{r+1,\dots,r+r'\}$. We obtain $F_z' = F_e' \cup F_r'$. In our study, recharging stations $i \in F_e \cup F_z'$ are defined with a recharging speed λ_i. Moreover, partial battery recharging is allowed at any station. The recharging time is proportional to the recharged energy, which is usually longer than the refueling time. Moreover, since the landfill facilities can be visited more than once, copies of landfill nodes are created. Thus, L' is the set of dummy vertices to allow multiple visits to each node in the set of L where $L' = \{l+1,\dots,l+l'\}$.

Using the defined sets and indies, the investigated problem is defined on a complete graph $G = (V \cup V', A)$, where $A = \{(i,j): i,j \in V \cup V', i \neq j\}$ is the set of arcs. The depot is also considered a refueling and charging station and belongs to the set F'_z, where vehicle routes should start and end. Since the depot is regarded as a refueling/recharging station, we duplicate the depot and denote by o and o' as the starting and ending nodes, respectively. For each arc $(i,j) \in A$, we associate a non-negative travel time t_{ij} and a distance d_{ij} ($d_{ij} = t_{ij}$). The recharging (refueling) stations and the landfill facility nodes allow operation at any time during the day. A mixed-integer non-linear program formulation of the HWCP is now presented. This mathematical formulation is inspired from the works of Kim et al. (2006) and Macrina et al. (2019).

Indices and sets

o	starting depot
o'	ending depot
B	set of customers
L	set of landfills
F_e	set of charging stations
F_r	set of refueling stations
F_z	set of power sources, where $F_z = F_e \cup F_r$
L	set of dummy landfills vertices
F_e'	set of dummy charging vertices
F_r'	set of dummy refueling vertices

F'_z set of dummy power sources vertices, where $F'_z = F_e' \cup F_r'$.

V set of all physical nodes where $V = \{B \cup L \cup F_z\}$

V' set of all dummy nodes where $V' = \{B \cup L' \cup F'_z\}$

A set of arcs

d_{ij} distance from i to j

t_i^- earliest start time at which the vehicle starts the service time at customer i

t_i^+ latest start time at which the vehicle starts the service time at customer i

q_i amount of waste at customer

t_{ij} time of arrival at node j from i

s_i service time at node i. If node i belongs to L, then s_i is the service time to empty the landfill.

       If node i belongs to F_r', then s_i is the refueling time at the refueling station.

R_{max} maximum route duration expressed by the total travel time, time of refueling and recharging time.

c_z cost rate associated with each fuel type

C maximum capacity payload of the vehicle

H^e battery capacity for the electricity

H^r tank capacity for the CNG fuel

λ_i recharging speed at each charging station $i \in F_e \cup F_e'$

Decision variables

x_{ij} binary variables equal to 1 if arc (i,j) is traveled by a vehicle and 0 otherwise.

B_i continuous variables represent the time at which the vehicle starts servicing node i.

Q_i continuous variables indicate the total waste carried on the vehicle immediately after visiting node i.

y_j continuous variables represent the remaining CNG in the tank upon arrival to node j.

u_{ij}^z binary variables equal to 1 if the vehicle traverses arc (i,j) using power type z, and 0 otherwise.

d_{ij}^z binary variables represent the distance traveled by a vehicle traveling arc (i,j) when power type z is

       selected. In this case, this variable takes the actual distance value d_{ij}, and 0, otherwise.

o_{ij} continuous variables represent the remaining energy in the battery of the vehicle upon arrival to node

       j from node i, with $(i,j) \in A$

g_{ij} continuous variables define the quantity of energy recharged from the recharging station node $i \in$

       $F_e \cup F_e'$ to travel at any node $j \in V'$

$$\text{minimize} \sum_{z \in e,r} \sum_{i \in V \cup V'} \sum_{j \in V \cup V', j \neq i} d_{ij}^z u_{ij}^z c_z \tag{8}$$

subject to

$$\sum_{j \in V \cup V'} x_{ij} = 1 \qquad\qquad \forall i \in B \tag{9}$$

$$\sum_{j \in V \cup V' \backslash \{t\}} x_{ij} = \sum_{j \in V \cup V' \backslash \{o\}} x_{ji} \qquad\qquad \forall i \in V \cup V' \tag{10}$$

$$\sum_{i \in V \cup V' i \neq t} x_{t,i} = \sum_{j \in V \cup V' j \neq o} x_{j,o} \qquad\qquad \forall i \in V \cup V' \tag{11}$$

$$B_j \geq B_i + (s_i + t_{ij}) x_{ij} - M(1 - x_{ij}) \qquad\qquad \forall i \in V \cup V', \forall j \in V \cup V' \backslash \{o,t\}, i \neq j \tag{12}$$

$$B_j \geq B_i + t_{ij} u_{ij}^e + \frac{1}{\lambda_i} p_{ij} - M(1 - u_{ij}^e) \qquad\qquad \forall i \in F_e \cup F_e', \forall j \in V' \tag{13}$$

$$0 \leq B_o \leq R_{\max} \tag{14}$$

$$B_j \leq R_{\max} - (s_j + t_{j,t}) \qquad\qquad \forall j \in V \cup V' \backslash \{o,t\} \tag{15}$$

$$t_i^- \leq B_i \leq t_i^+ \qquad\qquad \forall i \in V \tag{16}$$

$$Q_o = 0 \tag{17}$$

$$Q_t = 0 \tag{18}$$

$$Q_j \geq Q_j + q_j x_{ij} - C(1 - x_{ij}) \qquad\qquad \forall i \in V \cup V' \backslash \{o,t\}, \forall j \in V \cup V' \{o\} \tag{19}$$

$$Q_j \leq C \qquad\qquad \forall j \in V' \tag{20}$$

$$Q_i = 0 \qquad\qquad \forall i \in L' \tag{21}$$

$$\sum_{j \in B \cup F_z \cup F'_z} x_{ij} \geq 1 \qquad\qquad \forall i \in L \cup L' \tag{22}$$

$$\sum_{z \in e,r} d_{ij}^z \cdot u_{ij}^z = d_{ij} \qquad\qquad \forall i,j \in V \cup V' \tag{23}$$

$$\sum_{z \in e,r} u_{ij}^z \geq x_{ij} \qquad\qquad \forall i,j \in V \cup V' \tag{24}$$

$$y_i = H^r \qquad\qquad \forall i \in F_r \cup F_r' \tag{25}$$

$$y_j \leq y_i - FR_{ij}^r(Q_i) + H^r(1 - u_{ij}^r) \qquad\qquad \forall i,j \in V \cup V' \backslash \{t\} \tag{26}$$

$$0 \leq y_j \leq H^r \qquad\qquad \forall j \in V \cup V' \backslash \{t\} \tag{27}$$

$$o_{ij} \leq (o_{hj} + g_{ij}) - p_{ij}^e(Q_i) u_{ij}^e + M(1 - u_{ij}^e) + M(1 - u_{hi}^e) \qquad\qquad \forall h \in V', \forall i \in V \backslash \{o\}, \forall j \in V', i \neq j, i \neq h, j \neq h \tag{28}$$

$$o_{oj} \leq H^e - p_{oj}^e(Q_j) u_{oj}^e + M(1 - u_{oj}^e) \qquad\qquad \forall j \in V' \tag{29}$$

$$g_{ij} \leq H^e - o_{hi} + M(1 - u_{ij}^e) + M(1 - u_{hi}^e) \qquad\qquad \forall i \in F_e \cup F_e' \backslash \{o\}, \forall h \in V', \forall j \in V' \tag{30}$$

$$o_{ij} \geq 0.1H^e \qquad\qquad \forall i \in F_e \cup F_e', \forall j \in V' \tag{31}$$

$$g_{ij} \leq 0.9H^e \qquad\qquad \forall i \in F_e \cup F_e', \forall j \in V' \tag{32}$$

$$x_{ij} \in \{0,1\} \qquad\qquad \forall i,j \in V \cup V' \tag{33}$$

$$u_{ij}^z, d_{ij}^z \in \{0,1\} \qquad\qquad \forall z \in \{r,e\}, \forall i,j \in V \cup V' \tag{34}$$

$$y_i \geq 0 \qquad\qquad \forall i \in V \cup V' \tag{35}$$

$$B_i, Q_i \geq 0 \qquad\qquad \forall i \in V \cup V' \tag{36}$$

$$g_{ij} \geq 0 \qquad\qquad \forall i \in F_e \cup F_e', \forall j \in V'. \tag{37}$$

The objective function (8) optimizes the total routing costs of all vehicles. Constraints (9) guarantee that each customer must be served by only one vehicle. Constraints (10) define arc flows. Constraints (11) guarantee that each route vehicle starts and ends at the depot. Constraints (12) and (13) define arrival times, whereas (14) and (15) ensure that each vehicle returns to the depot no later than R_{max}. Time windows are defined in (16). Constraints (17) and (18) ensure that each vehicle leaves and returns with an empty load to the depot. Constraints (19) and (20) ensure vehicle capacity limitations. Constraints (21) set the weight of each vehicle

to zero after leaving a landfill station. In addition, constraints (19) and constraints (21) enforce that the vehicle must go to the landfill facility to be emptied when it is full. Constraints (22) ensure that a vehicle can visit the following location (customer or recharging/refueling station) or return from a landfill node to the depot. Constraints (23) guarantee that the distance from node i to j can be served by fuel type z. Constraints (24) ensure that one fuel type is used to travel from node i to node j. Constraints (25) ensure that the CNG fuel tank is reset to its maximum H^r after visiting each refueling CNG station. If i is a customer node and j is visited immediately after i, the first term of constraints (26) ensures that the CNG level is reduced when the vehicle arrives at j following the distance from i to j and the CNG consumption rate. Constraints (27) monitor the CNG fuel level. Constraints (28) and (29) guarantee that the battery capacity is respected, while constraints (30) model the partial recharging of the battery. Constraints (31) and (32) ensure the safe operation of the battery since full (100%) and empty (0%) charges can damage it. Finally, constraints (33)-(37) define the domains of decision variables.

We note that the formulation is only presented to provide a formal mathematical definition, but it cannot be used to solve small instances. As previously stated, it generalizes and jointly considers several subproblems such as the WCVRP, the HVRP, and considers intersection points, which are themselves known to be difficult to solve to optimality. Moreover, consumption functions are highly non-linear. Therefore, in the next section, a Hybrid Threshold Acceptance (HTA) algorithm is developed for the particular requirements of the HWCP to face the challenges imposed by the specific aspects of this problem.

5. Hybrid Threshold Acceptance algorithm for the HWCP

This section presents our HTA algorithm tailored as an effective solution methodology for the HWCP. The Threshold Acceptance (TA) algorithms have been proposed as an efficient tool to solve a variety of routing problems, see, e.g., Nikolakopoulos and Sarimveis (2007), Bräysy et al. (2008), Braekers et al. (2014).

The algorithm works as follows. Let x be an initial solution and x_{best} the current best solution. The threshold T is initialized to its maximum value defined by T_{max}. In a TA, a new solution x' is generated from x. If the objective value of x' ($f(x')$) is better than that of x, the new solution x' is accepted and, therefore, becomes a new solution in the next iteration. Otherwise, the solution x' is accepted if the difference in the objective function values calculated by $\Delta = f(x') - f(x)$ is less than the threshold value T. This value is reduced during the search until only improved solutions are accepted (Braekers et al., 2014).

There are two distinct advantages to using a TA algorithm as a solution methodology: 1) it is relatively easy to adapt for various types of optimization problems; and 2) it relies only on a single parameter (T), which makes the algorithm more robust and helps to reduce the burden of additional computational time, as in other advanced metaheuristic algorithms (see, e.g., Braekers et al., 2014). Moreover, the threshold acceptance function of the TA is less complex than the stochastic function of SA (Talbi, 2009). As far as we know, TA has not been considered in the literature to solve any WCVRPTW variants. Furthermore, we propose various modifications to improve the standard TA algorithm for the investigated problem.

One of the disadvantages of TA, especially when solving highly constrained optimization problems, is that it may get stuck in a local optimum and not be able to leave it. To overcome this, we focus on enhancing the

performance of the TA algorithm and its convergence to obtain high-quality solutions by using better diversification and intensification mechanisms.

The proposed HTA algorithm has unique features and differs from other methods because it considers the main advantages of several well-known metaheuristics. In the literature, the authors have proposed various hybridization techniques such Bees Algorithm in Masmoudi et al. (2016), Bee Colony in Masmoudi et al. (2019), or Adaptive Large Neighborhood Search algorithm in Masmoudi et al. (2020). The main structural difference between this work and others has been achieved by including new features from state-of-the-art evolutionary-based algorithms and other diversification and intensification components from single solution-based metaheuristic algorithms. The details are provided next.

The main focus of TA is to search repeatedly around a single feasible solution, reducing the chance of looking at other potential solutions. In our HTA algorithm, we restart *s* at each TA iteration from a different initial solution. We, therefore, look at a broader solution space during the search and avoid from unnecessary iterations around local optima. This multi-start approach has been used in various studied (e.g., Vincent and Lin, 2014; Koç et al., 2019; Masmoudi et al. , 2020). This is done by using the advantages of GA (the crossover and the ability to explore the search space (Masmoudi et al., 2020)). We build a new solution with the crossover operator of GA. A newly created solution is then used as the current solution for the subsequent iteration. This helps diversify the solution space.

Generally, a new solution is created from the current solution, using a randomly selected neighborhood operator from a random order of the set of neighborhood searches N_h, and this solution is either accepted or rejected. Then, the next operator is applied from the set of neighborhood search operators. This standard mechanism can also be further improved. In our HTA, we use the following procedure instead of switching to the next operator as in the traditional TA (even to accept or reject the new solution). First, a predefined order of all neighborhood searches to be used. Then, the current neighborhood from this order is applied to the current solution x. If the new solution x' is better than the current solution x, a new order is updated where the current neighborhood operator is switched to the first position. Otherwise, the next operator is applied. This technique is inspired from VND algorithms. This technique during the diversification phase provides a better solution quality than other ones obtained by standard methods (e.g., Karakostas and Sifalera, 2022).

An advantage of using different diversification procedures is to discover new regions of the search space that may not have been visited yet by the neighborhood search operators. Our method balances diversification and intensification mechanisms to handle hard optimization problems, as is the case of our problem. The proposed enhanced TA is not only tailored to address HWCP but can be regarded as a new generalized algorithmic framework.

Finally, a new speedup mechanism has been introduced to avoid unnecessary move evaluations and prevent the same search over a solution. This increases the runtime of the algorithm.

A sketch of our HTA algorithm is provided in Algorithm 1. Let att, initialized to one, be the counter for the multi-start step, i_{last} initialized to zero be used as a counter of the number of iterations when x_{best} is improved, a set of N_h neighborhood searches $h=\{1,\ldots, h_{max}\}$, x the initial solution, and x_{best} the current best solution that is initialized to x. The HTA runs until the stopping criterion has been met and returns the best solution x_{best}. Each run, except the first one, works as a multi-start step which calls the crossover operator.

13

Thus, a new solution is created, combining the current characteristics of x_{best} and a newly generated solution by the constructive heuristic (Section 4.1). A new solution x' is generated using the current neighborhood search N_h. In each iteration a re-ordering of the neighborhood operators is performed in descending order, based on the improvements achieved by applying each of them in each previous iteration. An initial predefined neighborhood order (from the most to the least complex) is adopted (line 3 of Algorithm 1). Next, for each diversification phase the neighborhood operators are successively selected according to their order (lines 15-19 of Algorithm 1), and the incumbent solution x is diversified (line 10 of Algorithm 1) to produce a new solution x'. Then, a local search operator (line 11 of Algorithm 1, Section 4.4) is applied to x' to provide an improved solution x''. Each local search is applied with speed-up mechanism Static Move Descriptor (SMD) (line 11 of Algorithm 1, Section 4.4).

After performing the neighborhood and local search operators, the solution may be infeasible due to fuel usage and vehicle capacity constraints. In this case, the following procedure is applied: first, the Remove Landfill (RL) and Insert Landfill (IL) operators are used to restore the feasibility with respect to capacity issues (line 12 of Algorithm 1); then, the Remove Fueling Station (RFS) and Insert Fueling Station (IFS) operators are performed to regain feasibility related to the fuel usage (line 13 of Algorithm 1). These procedures are described in Section 4.3. If the value of x'' is less than that of x' plus the threshold T, x'' is used as a new current solution. This allows better space exploration and provides a chance for each new solution x'' to become a promising solution during the search. In addition, if x'' is better than the current one obtained from our neighborhood search in Section 4.2, a new order neighborhood is updated (lines 15-19 of Algorithm 1) and the neighborhood N_h is changed to the first neighborhood N_1 according to its performance on the previous iterations (lines 21 in Algorithm 1); otherwise, N_h is changed to the next neighborhood (line 23 in Algorithm 1). Finally, if the value of x is better than that of x_{best}, x becomes the new best solution (line 25 of Algorithm 1). If no new best solution is obtained, the value of T is reduced by the threshold reduction parameter ΔT (lines 31-32 of Algorithm 1). If T becomes negative, its value is reset to $T_{max} * \beta$, where β is a randomly generated number between zero and one (lines 33-36 of Algorithm 1).

Algorithm 1: Hybrid Threshold Acceptance Algorithm

1. **Initialize**: $i_{last} = 0$ and $x = x_{best}$ = constructive heuristic; a set of neighborhood structures N_h, where $h = \{1, ..., h_{max}\}$; *InitialNeighborhoodOrder*;
2. **Repeat**
3.   *Order←InitialNeighborhoodOrder*   *// initialize the order*
4. $i_{last} \leftarrow i_{last} + 1$;   *//iterations without improvement*
5.   **If** *att >1* **Then**   *// multi-start approach*
6. $x_{new} \leftarrow$ a newly generated solution using the constructive heuristic;
7. $x \leftarrow$ Crossover(x_{best}, x_{new});   *//create a new solution*
8. $h \leftarrow 1$;   *//use neighborhood 1*
9.   **Repeat**
10.   Find a new solution x' from the hth neighborhood of x ($x' \in N_h(x)$);   *//generation of a new solution*
11. $x'' \leftarrow$ local search operator(x', SMD)   *// improve the solution*
12.   Apply the RL and IL operators on x'';   *//improve landfills*
13.   Apply the RFS and IFS operators on x'';   *//improve refuel/recharge*
14.   **If** $f(x') < f(x) + T$ **Then**
15.   **For** $i \leftarrow 1$ to h_{max} **Do**   *// Generate the new Order*
16. $l \leftarrow$ neighborhood with high improvement number;
17.   *UpdateOrder(i)* $\leftarrow l$;
18.   **End For**
19.   *Order←UpdateOrder*;
20. $x \leftarrow x'$;   *//update the current solution*

21	$h \leftarrow 1;$	//use neighborhood 1 based on *Order*
22	**Else**	
23	$h \leftarrow h + 1;$	//use next neighborhood
24	**If** $f(x) < f(x_{best})$ **then**	
25	$x_{best} \leftarrow x;$	//new best solution
26	$i_{last} \leftarrow 0;$	
27	$x_{best} \leftarrow f(x_{best});$	
28	**End if**	
29	**Until** $h = h_{max} + 1$	
30	$att = att + 1;$	
31	**If** $i_{last} > 0$ **then**	
32	$T \leftarrow T - \Delta T$	//update threshold
33	**If** $T < 0$ **then**	
34	$\beta \leftarrow$ Random number from the interval [0,1];	
35	$T \leftarrow \beta \times T_{max};$	
36	**End if**	
37	**End if**	
38	**Until** the run time is reached	
39	**Return** x_{best}	

5.1. Constructive heuristic

We propose an enhanced version of the insertion heuristic used by Masmoudi et al. (2018b). Additionally, we consider new features, such as fuel consumption (electricity and CNG) and multiple visits to landfill facilities.

For the first feasible solution, a list L with a set of customers is created. A customer (i) is randomly selected from the list and inserted back into the existing route in the best position. This selection must satisfy time windows and maximum route duration constraints. The nearest landfill facility is inserted before node i if the accumulated waste at node i exceeds the vehicle's capacity. If a new customer i cannot be visited due to limited fuel constraints, the selected customer is reinserted after the fuel recharging (refilling) node station. This is done by selecting the fueling station closest to the current node and inserting it between the previously inserted customer and the current customer node i. We note that at each visited CNG station, the fuel tank is refueled to its maximum capacity, while at a recharging station partial recharging is allowed. This is done by recharging the battery as much as necessary to visit the next node. Because the recharging time is much longer than the refueling time, the impact on time windows and maximum route duration must be considered. If they are respected and some customers are not serviced, a new route is created, and the same insertion procedure is run until all customers have been visited.

5.2. Neighborhood structures

The order of neighborhood search structure is the main key to the success of our HTA, as indicated in several VNS variants (Mladenović and Hansen, 1997). We propose four effective neighborhood search structures with various movement tactics based on Masmoudi et al. (2018b), as described below. The neighborhood searches N1 and N2 perform a small perturbation to the solution while N3 and N4 perform a higher perturbation to the incumbent solution.

Swap-Exchange (**N1**): This operator swaps a random node selected from one route with another one from any route.

Removing-insertion (**N2**): This neighborhood operator is similar to a greedy procedure. This move consists of randomly choosing two routes. Then, from each one, a sequence (seq) of consecutive nodes is selected. All

nodes forming the selected sequences (including the refueling and recharging nodes) are then removed and reinserted at their best positions on the other route. When inserting a node, the algorithm checks all possible combinations of insertion positions of the node on the current route. Nevertheless, each of these new routes can violate fuel-related constraints. In this case, a refueling or recharging station node is also inserted at its best position. The value of seq is selected randomly between one and five.

Cross-exchange **(N3)-(N4)**: In this move, we exchange nodes between two routes. First, b consecutive nodes are transported from one route to another. Afterwards, d consecutive nodes are transported from route two to route one. The selection of b is limited to two and three, and d is randomly chosen as b or b-1, as the chance of having an effective swap is minimized with longer segment lengths. We limit the segment length to two (**N3**) and three (**N4**). Considering its capacity for effective diversification, this operator is mainly used at the perturbation stage (Hemmelmayr et al., 2009; Masmoudi et al., 2018b).

At the end of the neighborhood and local search operators, redundant refueling, recharging, and landfill facility node visits might occur. Moreover, the current solution may require visiting refueling or recharging stations and landfill facility nodes. For these reasons, two operators related to the landfill facility and two operators related to fueling are proposed in the next section.

5.3. Feasibility regain procedures

To maintain the feasibility of the solution in terms of landfill and refuel/recharge constraints, we use two operators for the landfill constraints (Remove Landfill (RL) and Insert Landfill (IL)) and two for the refuel/recharge constraints (Remove Fueling Stations (RFS) and Insert Fueling Station (IFS)). These operators are described below.

Remove Landfill **(RL)**: The RL is performed at each route of a solution. The idea of this operator is to verify for every landfill facility visit if the total collected waste does not violate the capacity vehicle at the next node after the landfill. In this case, the landfill facility node is deleted.

Insert Landfill **(IL)**: The RL considers all nodes i and j of each route ($\forall\ i, j\ \in B$), such that if the total amount of waste at node j violates the capacity vehicle, a landfill facility is inserted prior to it. It is done by finding the closest landfill node to node i. After a visit to the landfill facility, the capacity of a vehicle is reset to zero.

Remove Fueling Station **(RFS)**: The RFS is similar to the RL operator. It investigates for every fueling station visit if the fueling (electric or CNG station) node can be removed such that the amount of fuel (electricity and CNG) is sufficient to reach the next node of the route.

Insert Fueling Station **(IFS)**: For each node $i \in B \cup L$, if the remaining fuel in a tank and the charge level in a battery at node i are not sufficient to reach the next node directly or to reach the closed station after that, a visit to the station closed to i is performed. Starting at node i, the operator assumes that the remaining battery and CNG fuel at node i are sufficient to reach the nearest station. This is done by calculating the current power type that needs to be used between the current node i and all recharge and refueling station nodes.

5.4. Intensification mechanisms

Four well-known local search operators are proposed to quickly and efficiently improve the solution obtained from the current neighborhood. We use two intra-route operators (relocate of Savelsbergh (1992) and

2-opt of Lin (1965)) and two inter-route operators (remove two insert one of Xiang et al. (2006) and relocate of Savelsbergh (1992)).

These operators are computationally expensive. To improve the runtime, a speed-up mechanism is implemented.

Static Move Descriptor (SMD): This mechanism is similar to the work of Beek et al. (2018). For a given route or pair of routes, we first determine the best-improving move of a particular neighborhood. We then store the information. If there is no improvement, we also store this information. At the start of the search, the algorithm verifies whether the given route or pair of routes have already been explored. Then, the SMD returns the information of the best-improving move or that there is no such move. If not, the search is performed normally, and it stores the corresponding information regarding the route or pair of routes.

6. Numerical Experiments

We now present the detailed numerical results. We have implemented the HTA algorithm in the C programming language on a system with an Intel Core i5-10310U processor running at 1.70 GHz with 8 GB RAM.

We apply the HTA algorithm on a new set of instances generated as no benchmark publicity is available. We have adapted the well-known EVRP benchmark instances. For these instances, three sets are denoted as C, R, and RC, created by Schneider et al. (2014).

We set the numbers e and r of stations based on the number of customers in each instance in our data set. For b customers, the number of refueling stations (CNG) and recharging stations are assumed to be $0.1*b$, as done in Goeke and Schneider (2015), for each type of station. The coordinates of these nodes are randomly generated on a specific square area (i.e., $[-10, 10]^2$). We note that the depot is also considered a refueling and recharging station. The number of landfill nodes is between two and three, also randomly generated.

To consider the characteristics of different technologies, we assumed that the charging stations in the network are homogeneous. With this assumption, vehicles can be charged at any available station at the same cost and charging time. While different charging stations exist in reality, we have followed the work of Macrina et al. (2019) and considered only one type, i.e., recharging at 20,000 KWh/h.

Finally, our adapted instances consider various levels of road gradients between -6% and 6% (Masmoudi et al., 2018b). The detailed instances and results can be found on the following website: https://hwcvrp-45.webself.net/.

In Section 6.1 we describe the parameter setting of our algorithm, and in Section 6.2 we assess the performance of our algorithm on the classical EVRP instances from the literature and perform a sensitivity analysis of the different elements of our algorithm on these results. In Section 6.3, we use the modified EVRP instances with new recharging stations and test the performance of our algorithm on our HWCP, where we test the performance of different consumption rates and energy usage.

6.1. Parameter setting

We now provide the results of sensitivity analyses. The initial values of the parameters are determined based on previous experiments conducted in the literature. The performance of our HTA algorithm has a strong relationship with these parameters, and we fine-tune them as follows.

The main TA parameter is the maximum threshold value (T_{max}) (Braekers et al., 2014). Based on Braekers et al. (2014) and Masmoudi et al. (2018a), T_{max} should be less than five. Based on preliminary tests, we set T_{max}=4. To assess the influence of this parameter, we tested our HTA algorithm on 20 large-sized instances, which were selected with various features. All experiments are run ten times on each instance.

To tune parameters, the following procedure was performed. First, we fix the runtime (i.e., 10, 20, and 30 minutes). Second, for each fixed runtime, we evaluate the robustness of different T_{max} values (i.e., 2; 2.5; 3; 3.5; 4). Table 2 provides the sensitivity analysis results for the parameter T_{max}. The column denoted "Best" ("Avg") represents the average over all 20 instances of the best (average) solution value obtained by our HTA for each corresponding parameter combination.

Table 2 Identification of the best parameters setting for the HTA algorithm

T_{max}	10 minutes					20 minutes					30 minutes				
	2	2.5	3	3.5	4	2	2.5	3	3.5	**4**	2	2.5	3	3.5	4
Best	1915.43	1914.26	1912.59	1910.90	1910.52	1894.64	1892.92	1891.22	1890.87	**1890.11**	1890.37	1889.38	1889.14	1888.67	1888.39
Avg	1922.94	1922.26	1920.29	1918.11	1917.20	1906.41	1902.47	1897.78	1898.54	**1897.14**	1896.90	1896.49	1896.24	1896.14	1895.70

Table 2 shows that no significant improvement has been achieved in average solution values after 20 minutes. The quality of best and average solutions slightly improves when using T_{max}=4 and 30 minutes, but we consider that the gains are not worth the extra time. The results shown in Table 2 suggest that T_{max} should be four. To balance solution quality and runtime for instances of different sizes, we stop the algorithm after 10 consecutive iterations without improving the best solution. This choice also follows that of Masmoudi et al. (2016).

6.2. Analysis on EVRP(-PR) benchmark instances

To further demonstrate the efficiency of our HTA algorithm, EVRP benchmark instances are solved. By considering only electricity as the energy source in our fleet and by relaxing the constraints related to the landfills, our problem can be easily transformed into an EVRP-PR. The objective function aims to minimize the number of vehicles used and decrease the total distance.

The state-of-the-art algorithm for this problem, namely the hybrid ILS of Cortés-Murcia et al. (2019), presents the most recent method to solve the EVRP-PR, and is compared with our HTA algorithm. We also list all the best-known solutions and the papers that obtained them. Table 3 compares our algorithm against the hybrid ILS of Cortés-Murcia et al. (2019) on the EVRP-PR instances. Column "BKS" refers to the best-known solution, while "Best (%)" and "Avg (%)" are the percentage deviations from the best known (average) solution obtained in ten runs. We also present CPU times in minutes. Our algorithm stops when there is no improvement of the best solution after ten consecutive iterations. This stopping condition is inspired by Masmoudi et al. (2016) and intends to obtain a good quality solution.

It should also be noted that we cannot compare the performance of the algorithms to the computational time reported in Cortés-Murcia et al. (2019). This is because a different machine has been used to run our algorithms than that used for the hybrid ILS. Moreover, the speed factor of the configuration applied on HTA cannot be estimated by using Dongarra's (2014) results due to a lack of relevant information in Dongarra (2014) and Linpack (www.roylongbottom.org.uk).

Table 3
Comparison of our HTA with the hybrid ILS of Cortés-Murcia et al. (2019) on EVRP-PR instances

Inst.	Nb_Veh	BKS	Hybrid ILS[Cortés-Murcia et al., 2019][a]				HTA			
			Nb_Veh	Best	Best%	CPU (min)	Nb_Veh	Best	Best%	CPU (min)
c101	12	1043.38[c]	12	1043.38	0.00	1.12	12	1043.38	0.00	2.68
c102	11	1017.7[b]	11	1017.70	0.00	1.46	11	1017.70	0.00	4.14
c103	10	971.19[b]	10	971.19	0.00	2.08	10	971.19	0.00	1.39
c104	10	884.38[d]	10	884.38	0.00	1.72	10	884.38	0.00	2.76
c105	11	1015.79[b]	11	1015.79	0.00	1.25	11	1015.79	0.00	2.07
c106	11	1009.33[b]	11	1009.33	0.00	1.42	11	1009.33	0.00	1.38
c107	10	1046.50[b]	10	1046.50	0.00	1.85	10	1046.50	0.00	1.74
c108	10	1022.48[b]	10	1022.48	0.00	1.99	10	1022.48	0.00	5.68
c109	10	940.38[c]	10	940.38	0.00	2.28	10	940.38	0.00	2.35
c201	4	629.95[d]	4	629.95	0.00	1.11	4	629.95	0.00	2.91
c202	4	629.95[d]	4	629.95	0.00	1.47	4	629.95	0.00	3.36
c203	4	629.95[d]	4	629.95	0.00	1.91	4	631.97	0.32	4.24
c204	4	628.91[d]	4	628.91	0.00	2.29	4	628.91	0.00	1.83
c205	4	629.95[d]	4	629.95	0.00	1.41	4	629.95	0.00	4.85
c206	4	629.95[d]	4	629.95	0.00	1.65	4	629.95	0.00	1.53
c207	4	629.95[d]	4	629.95	0.00	1.73	4	629.95	0.00	2.54
c208	4	629.95[d]	4	629.95	0.00	1.71	4	629.95	0.00	5.01
r101	18	1606.98[b]	18	1606.98	0.00	2.49	18	1606.98	0.00	4.92
r102	15	1461.23[b]	15	1461.23	0.00	2.68	15	1470.00	0.60	3.65
r103	13	1212.37[b]	13	1212.37	0.00	2.81	13	1214.31	0.16	4.50
r104	11	1051.41[b]	11	1051.41	0.00	3.09	11	1054.56	0.30	2.08
r105	14	1347.80[c]	14	1362.31	1.08	2.77	14	**1359.39**	**0.86**	1.97
r106	13	1256.19[b]	13	1256.19	0.00	2.76	13	1256.19	0.00	4.34
r107	12	1108.47[b]	12	1108.47	0.00	2.56	12	1108.47	0.00	4.53
r108	11	1020.52[b]	11	1020.52	0.00	3.01	11	1020.52	0.00	1.82
r109	12	1185.77[b]	12	1185.77	0.00	3.24	12	1185.77	0.00	3.46
r110	11	1070.99[c]	11	1071.92	0.09	3.18	11	**1071.42**	**0.04**	3.07
r111	11	1072.46[b]	11	1072.46	0.00	3.25	11	1078.79	0.59	5.61
r112	11	1001.79[c]	11	1001.79	0.00	3.22	11	1001.79	0.00	2.50
r201	3	1255.81[b]	3	1255.81	0.00	3.04	3	1255.81	0.00	3.12
r202	3	1051.46[c]	3	1051.46	0.00	2.23	3	1056.72	0.50	8.92
r203	3	895.54[d]	3	895.54	0.00	2.73	3	895.54	0.00	2.95
r204	2	780.91[b]	2	780.91	0.00	4.44	2	781.93	0.13	6.25
r205	3	987.22[b]	3	987.22	0.00	2.56	3	987.22	0.00	10.21
r206	3	922.70[d]	3	922.70	0.00	2.62	3	922.70	0.00	15.60
r207	2	843.20[c]	2	857.07	1.64	3.61	2	**851.72**	**1.01**	9.41
r208	2	736.12[d]	2	738.84	0.37	3.38	2	742.01	0.80	5.72
r209	3	863.36[c]	3	870.68	0.85	2.49	3	871.39	0.93	3.46
r210	3	843.36[d]	3	846.62	0.39	2.34	3	849.09	0.68	3.37
r211	2	826.88[c]	2	826.88	0.00	3.79	2	826.88	0.00	2.80
rc101	15	1648.99[d]	15	1661.53	0.76	2.62	15	**1654.27**	**0.32**	5.38
rc102	14	1510.16[c]	14	1510.16	0.00	2.58	14	1510.16	0.00	7.65
rc103	12	1346.83[b]	12	1346.83	0.00	2.62	12	1350.60	0.28	4.60
rc104	11	1175.06[c]	11	1175.83	0.07	2.70	11	1180.47	0.46	7.69
rc105	14	1446.30[b]	14	1446.30	0.00	2.55	14	1446.30	0.00	5.67
rc106	13	1383.14[b]	13	1383.14	0.00	2.68	13	1383.14	0.00	5.35
rc107	12	1244.83[b]	12	1244.83	0.00	2.63	12	1246.70	0.15	3.73
rc108	11	1154.14[c]	11	1159.90	0.50	2.48	11	1161.30	0.62	6.16
rc201	4	1443.07[b]	4	1443.07	0.00	2.34	4	1443.65	0.04	4.06
rc202	3	1403.32[b]	3	1403.32	0.00	3.27	3	1403.32	0.00	7.65
rc203	3	1060.32[c]	3	1068.28	0.75	3.04	3	**1066.47**	**0.58**	10.25
rc204	3	884.75[c]	3	884.97	0.02	2.94	3	888.55	0.43	4.81
rc205	3	1249.56[b]	3	1249.56	0.00	4.13	3	1254.43	0.39	8.30

rc206	3	1187.40[b]	3	1187.40	0.00	3.22	3	1188.35	0.08	2.98	
rc207	3	985.67[c]	3	996.63	1.11	3.36	3	**994.15**	**0.86**	18.28	
rc208	3	833.12[c]	3	833.12	0.00	3.17	3	834.87	0.21	5.82	
Avg	*-*	*1247.77*	*7.77*	*1043.39*	*0.14*	*2.55*	*-*	*1044.06*	*0.20*	*4.88*	

[a] Results of Cortés-Murcia et al.(2019), programmed in C++ and executed on 2.3 GHz Intel Xeon with 8 GB RAM
[b] Best-known solution provided by Cortés-Murcia et al.(2019)
[c] Best-known solution provided by Hiermann et al.(2019)
[d] Best-known solution provided by Keskin and Çatay (2016)

Observing the tested EVRP-PR instances, the quality solution obtained by our HTA is very close to that of the hybrid ILS of Cortés-Murcia et al. (2019) with a small gap. The HTA has an average deviation (Best%) of 0.20% which ranges between 0.00% and 1.01% from the BKS, while it is 0.14% for the hybrid ILS (ranging between 0.00% and 1.64%). This can explain the slightly more robust solutions of the hybrid ILS with a partial recharging policy to solve the EVRP-PR. Our proposed HTA can find BKS results in 31 instances compared to 44 among 56 instances. In addition, the HTA can find five better solutions than the hybrid ILS, as shown in bold. Thus, we can see that our HTA provides good results against the hybrid ILS of Cortés-Murcia et al. (2019).

Similar to the previous comparison, we compare our algorithm on the EVRP with full recharging benchmark instances where the battery is recharged to its maximum at each visit to the recharging station. In Table 4, we report the comparison of our algorithm against the hybrid GA of Hiermann et al. (2019). All columns of Table 4 have the same titles and meanings as in Table 3.

Table 4
Comparison of our HTA with the hybrid GA of Hiermann et al. (2019) on EVRP with full recharging instances

Inst	BKS	Veh	Hybrid GA [Hiermann et al., 2019][a]							HTA						
			Avg	Avg%	Veh	Best	Best%	Veh	CPU (min)	Avg	Avg%	Veh	Best	Best%	Veh	CPU (min)
c101	1053,83[b]	12	1053,83	0,00	12	1053,83	0,00	12	3,81	1053,83	0,00	12	1053,83	0,00	12	1,75
c102	1051,38[b]	11	1057,45	0,58	11	1055,12	0,36	11	5,37	1055,38	0,38	11	1052,64	0,12	11	2,51
c104	951,57[c]	10	958,91	0,77	10	953,63	0,22	10	10,07	951,57	0,00	10	951,57	0,00	10	3,32
c105	1075,37[b]	11	1076,71	0,12	11	1075,37	0,00	11	4,65	1078,38	0,28	11	1077,74	0,22	11	1,75
c106	1057,65[b]	11	1058,17	0,05	11	1057,65	0,00	11	5,25	1059,24	0,15	11	1057,65	0,00	11	3,02
c107	1031,56[b]	11	1033,44	0,18	11	1031,56	0,00	11	7,00	1032,80	0,12	11	1031,56	0,00	11	1,60
c109	1033,67[b]	10	1044,71	1,07	10	1060,78	2,62	11	11,26	1045,35	1,13	10	1043,49	0,95	11	6,55
c201	645,16[b]	4	645,16	0,00	4	645,16	0,00	4	5,38	645,16	0,00	4	645,16	0,00	4	5,22
c202	645,16[b]	4	645,16	0,00	4	645,16	0,00	4	7,59	645,16	0,00	4	645,16	0,00	4	4,28
c203	644,98[b]	4	645,00	0,00	4	644,98	0,00	4	7,93	646,46	0,23	4	644,98	0,00	4	4,90
c204	636,43[b]	4	636,92	0,08	4	636,43	0,00	4	8,57	641,97	0,87	4	638,91	0,39	4	4,98
c205	641,13[b]	4	641,13	0,00	4	641,13	0,00	4	6,46	641,77	0,10	4	641,13	0,00	4	5,02
c206	638,17[b]	4	638,17	0,00	4	638,17	0,00	4	7,32	638,17	0,00	4	638,17	0,00	4	3,64
c207	638,17[b]	4	638,17	0,00	4	638,17	0,00	4	7,56	638,17	0,00	4	638,17	0,00	4	4,20
c208	638,17[b]	4	638,17	0,00	4	638,17	0,00	4	7,54	638,17	0,00	4	638,17	0,00	4	4,54
r101	1663,04[b]	18	1664,50	0,09	18	1663,04	0,00	18	7,74	1672,35	0,56	18	1670,02	0,42	18	4,16
r102	1484,57[d]	16	1486,99	0,16	16	1484,57	0,00	16	7,95	1487,69	0,21	16	1484,57	0,00	16	2,62
r103	1268,88[d]	13	1284,47	1,23	13	1268,88	0,00	13	11,89	1268,88	0,00	13	1268,88	0,00	13	3,04
r104	1088,43[b]	11	1090,68	0,21	11	1103,50	1,38	11	14,74	1095,18	0,62	11	1093,33	0,45	11	2,68
r107	1148,38[d]	12	1163,54	1,32	12	1148,38	0,00	12	13,78	1158,72	0,90	12	1155,27	0,60	12	2,33
r108	1049,12[d]	11	1064,58	1,47	11	1049,12	0,00	11	15,23	1052,69	0,34	11	1049,12	0,00	11	1,59
r111	1099,53[d]	12	1111,12	1,05	12	1099,53	0,00	12	14,72	1101,18	0,15	12	1099,53	0,00	12	1,71
r112	1016,63[d]	11	1023,78	0,70	11	1016,63	0,00	11	14,25	1016,63	0,00	11	1016,63	0,00	11	3,18
r201	1264,82[b]	3	1273,88	0,72	3	1267,14	0,18	3	9,81	1268,74	0,31	3	1264,82	0,00	3	3,81
r202	1052,32[b]	3	1053,45	0,11	3	1052,32	0,00	3	10,96	1052,32	0,00	3	1052,32	0,00	3	5,81
r203	895,54[c]	3	910,15	1,63	3	895,54	0,00	3	12,35	901,36	0,65	3	898,76	0,36	3	4,63
r204	779,49	2	795,91	2,11	2	784,77	0,68	2	19,19	783,78	0,55	2	782,37	0,37	2	5,25
r205	987,36[c]	3	995,02	0,78	3	987,36	0,00	3	11,51	993,48	0,62	3	990,12	0,28	3	7,42
r206	922,19	3	932,97	1,17	3	925,34	0,34	3	14,18	925,14	0,32	3	923,30	0,12	3	3,94
r207	845,26	2	851,73	0,77	2	847,59	0,28	2	18,08	849,06	0,45	2	846,19	0,11	2	7,63

r208	736,12	2	739,11	0,41	2	736,12	0,00	2	17,26	742,67	0,89	2	738,77	0,36	2	6,00
r209	867,05	3	873,64	0,76	3	870,68	0,42	3	16,82	869,56	0,29	3	868,35	0,15	3	5,46
r210	846,62[c]	3	850,48	0,46	3	846,62	0,00	3	17,86	850,60	0,47	3	846,62	0,00	3	7,62
r211	827,89	2	834,94	0,85	2	836,27	1,01	2	19,45	835,09	0,87	2	834,18	0,76	2	5,38
rc101	1723,79[d]	16	1723,79	0,00	16	1723,79	0,00	16	13,02	1723,79	0,00	16	1723,79	0,00	16	4,93
rc103	1350,09	13	1350,98	0,07	13	1350,55	0,03	13	14,86	1351,44	0,10	13	1350,09	0,00	13	2,74
rc104	1227,25	11	1235,85	0,70	11	1230,92	0,30	11	13,46	1236,09	0,72	11	1229,21	0,16	11	3,57
rc105	1473,24[c]	14	1476,84	0,24	14	1473,24	0,00	14	12,13	1473,24	0,00	14	1473,24	0,00	14	3,79
rc106	1423,27[d]	13	1433,67	0,73	13	1423,27	0,00	13	9,81	1425,36	0,15	13	1423,27	0,00	13	1,72
rc107	1274,41[d]	12	1278,56	0,33	12	1274,41	0,00	12	13,72	1282,69	0,65	12	1274,41	0,00	12	2,67
rc108	1197,41[d]	11	1203,61	0,52	11	1197,41	0,00	11	8,92	1199,92	0,21	11	1197,41	0,00	11	2,46
rc201	1444,94[b]	4	1454,23	0,64	4	1446,03	0,08	4	10,10	1456,93	0,83	4	1452,60	0,53	4	4,44
rc202	1410,74[b]	3	1430,52	1,40	3	1421,34	0,75	3	11,78	1421,46	0,76	3	1415,25	0,32	3	5,37
rc203	1055,19	3	1069,15	1,32	3	1057,16	0,19	3	11,52	1057,62	0,23	3	1055,19	0,00	3	6,40
rc204	884,72[d]	3	888,20	0,39	3	884,72	0,00	3	13,12	891,00	0,71	3	886,31	0,18	3	5,27
rc206	1188,63	3	1209,22	1,73	3	1190,50	0,16	3	11,11	1195,29	0,56	3	1188,63	0,00	3	6,46
rc207	985,03	3	1002,13	1,74	3	991,96	0,70	3	12,78	989,17	0,42	3	986,02	0,10	3	7,61
rc208	836,29[d]	3	839,99	0,44	3	836,29	0,00	3	15,23	839,72	0,41	3	836,29	0,00	3	7,04
Avg	*1035,43*	-	*1041,85*	*0,61*	-	*1037,51*	*0,20*	-	*11,36*	*1039,18*	*0,36*	-	*1036,94*	*0,14*	-	*4,29*

[a] *Results of Hiermann et al. (2019), programmed in Java and executed on 3.3 GHz Intel Xeon with 4 GB RAM*
[b] *Best-known solution provided by Schneider et al.(2014)*
[c] *Best-known solution provided by Goeke and Schneider(2015)*
[d] *Best-known solution provided by Hiermann et al.(2019)*

Table 4 shows that our HTA is competitive against the hybrid GA of Hiermann et al. (2019) and provides good results on the EVRP with full recharging. Based on the number of best solutions (column Best), it is clear that our HTA outperforms the hybrid GA of Hiermann et al. (2019) by providing 16 best solutions compared to 9 for their hybrid GA. Considering the number of best average solutions found over ten runs (column Avg), our proposed HTA can also provide good results with 24 best average solutions compared to 17 for the hybrid GA. Regarding the average deviation of the best result (column Best), our HTA is slightly more efficient than the hybrid GA, with an average gap equal to 0.14%, compared to 0.20% obtained by the hybrid GA. The same holds for the average deviation of the average results from the best-known solutions (column Avg), where our HTA is also slightly more efficient with a gap of 0.36% compared to 0.61% by their hybrid GA.

We now present the impact of different components, i.e., different diversification and intensification mechanisms such as the multi-start approach, using the shaking phase of the VNS framework, and the updated order of the neighborhood search structures on the solution quality. To this end, new configurations are compared to the standard TA found in the literature (e.g., Nikolakopoulos and Sarimveis, 2007; Bräysy et al., 2008) by incorporating different component(s) each time. The detailed results are shown in Table 5, where the benchmark EVRP instances of Schneider et al. (2014) are used. First, in configuration "C1", we apply the standard TA described early in Section 5. Configuration "C2" represents the traditional TA with the multi-start approach (lines 5-7 of Algorithm 1). Configuration "C3" represents the traditional TA with the shaking phase procedure. In "C4", we apply our updating order of the different neighborhood structures into configuration C3 (lines 15-19 of Algorithm 1). Configuration "C5" combines C2 and C3. The last configuration, "C6", reflects our HTA described in Algorithm 1, in which we use all the components of the multi-start, updating neighborhood search order, and the shaking phases. Table 5 recapitulates these different configurations.

Table 5

A list of different configurations of the algorithmic components

Configuration	Description
C1	Traditional TA
C2	Traditional TA + multi-start approach
C3	Traditional TA + shaking phase procedure
C4	Traditional TA + shaking phase procedure+ update order of neighborhood structures
C5	Traditional TA + multi-start approach + shaking phase procedure
C6 (HTA)	Traditional TA + multi-start approach + shaking phase procedure+ update order of neighborhood structures (over algorithm)

Table 6 provides in columns "Best%" and "Avg%" the deviation gap from the Best-Known Solutions (BKS) on the EVRP-PR.

Table 6

Impact of different components on the solution quality

Inst.	BKS	Hybrid ILS of Cortés-Murcia et al. (2019) Best	Best (%)	C1 Avg (%)	Best (%)	C2 Avg (%)	Best (%)	C3 Avg (%)	Best (%)	C4 Avg (%)	Best (%)	C5 Avg (%)	Best (%)	C6 (HTA) Avg (%)	Best (%)
c101	1043.38[c]	1043.38	0.00	3.84	2.06	2.27	1.22	1.66	0.89	1.15	0.53	0.80	0.37	0.00	0.00
c102	1017.7[b]	1017.70	0.00	6.22	1.83	3.48	1.02	2.46	0.72	1.64	0.40	1.09	0.27	0.00	0.00
c103	971.19[b]	971.19	0.00	6.65	1.95	3.81	1.12	2.73	0.80	1.85	0.46	1.25	0.31	0.00	0.00
c104	884.38[d]	884.38	0.00	2.71	1.50	1.49	0.83	1.05	0.58	0.69	0.32	0.45	0.21	0.00	0.00
c105	1015.79[b]	1015.79	0.00	3.51	2.54	2.00	1.45	1.43	1.04	0.97	0.59	0.66	0.40	0.00	0.00
c106	1009.33[b]	1009.33	0.00	2.38	1.68	1.33	0.94	0.94	0.66	0.62	0.37	0.41	0.25	0.00	0.00
c107	1046.50[b]	1046.50	0.00	3.82	2.79	2.19	1.60	1.56	1.14	1.06	0.65	0.72	0.44	0.00	0.00
c108	1022.48[b]	1022.48	0.00	3.59	2.02	2.19	1.23	1.63	0.92	1.15	0.56	0.81	0.40	0.00	0.00
c109	940.38[c]	940.38	0.00	5.45	4.68	3.09	2.65	2.20	1.89	1.48	1.07	0.99	0.72	0.89	0.00
c201	629.95[d]	629.95	0.00	2.70	1.23	1.65	0.75	1.22	0.56	0.87	0.34	0.62	0.24	0.00	0.00
c202	629.95[d]	629.95	0.00	1.29	0.07	0.73	0.04	0.51	0.03	0.34	0.02	0.23	0.01	0.21	0.00
c203	629.95[d]	629.95	0.00	2.90	1.47	1.70	0.86	1.23	0.63	0.85	0.37	0.59	0.25	0.53	0.32
c204	628.91[d]	628.91	0.00	3.65	2.08	2.07	1.18	1.47	0.84	0.99	0.48	0.67	0.32	0.59	0.00
c205	629.95[d]	629.95	0.00	3.20	0.25	1.93	0.15	1.43	0.11	1.00	0.07	0.70	0.05	0.64	0.00
c206	629.95[d]	629.95	0.00	2.50	0.93	1.42	0.53	1.01	0.38	0.68	0.21	0.46	0.14	0.41	0.00
c207	629.95[d]	629.95	0.00	2.00	0.83	1.14	0.47	0.81	0.34	0.55	0.19	0.37	0.13	0.33	0.00
c208	629.95[d]	629.95	0.00	4.99	2.61	2.96	1.55	2.16	1.13	1.50	0.67	1.04	0.47	0.94	0.00
r101	1606.98[b]	1606.98	0.00	2.29	1.02	1.30	0.58	0.92	0.41	0.62	0.23	0.42	0.16	0.37	0.00
r102	1461.23[b]	1461.23	0.00	6.73	4.52	4.45	2.60	3.20	1.87	2.18	1.08	1.48	0.73	1.02	0.60
r103	1212.37[b]	1212.37	0.00	6.48	4.48	3.84	2.65	2.80	1.94	1.94	1.15	1.34	0.79	0.80	0.16
r104	1051.41[b]	1051.41	0.00	7.44	4.68	4.47	2.81	3.29	2.07	2.30	1.24	1.61	0.87	1.46	0.30
r105	1347.80[c]	1362.31	1.08	7.94	3.98	4.67	2.34	3.40	1.90	2.35	1.50	1.62	1.21	1.46	**0.86**
r106	1256.19[b]	1256.19	0.00	6.19	3.02	3.63	1.77	2.63	1.28	1.81	0.75	1.25	0.52	0.90	0.00
r107	1108.47[b]	1108.47	0.00	6.17	3.52	4.38	2.15	3.26	1.60	2.31	0.98	1.64	0.69	0.32	0.00
r108	1020.52[b]	1020.52	0.00	5.70	3.25	4.58	1.93	3.36	1.42	2.33	0.84	1.62	0.59	0.65	0.00
r109	1185.77[b]	1185.77	0.00	5.18	4.01	4.07	2.27	2.89	1.61	1.94	0.91	1.30	0.61	0.90	0.00
r110	1070.99[c]	1071.92	0.09	6.07	3.76	3.65	2.26	2.69	1.67	1.89	1.00	1.32	0.70	1.20	**0.04**
r111	1072.46[b]	1072.46	0.00	8.62	5.51	5.18	3.31	3.81	2.44	2.67	1.46	1.87	1.02	1.68	0.59
r112	1001.79[c]	1001.79	0.00	7.23	3.69	4.37	2.23	3.23	1.65	2.27	1.00	1.60	0.70	0.44	0.00
r201	1255.81[b]	1255.81	0.00	6.74	3.60	4.08	2.18	3.02	1.61	2.12	0.98	1.49	0.69	0.20	0.00
r202	1051.46[c]	1051.46	0.00	2.81	1.38	1.71	0.84	1.27	0.62	0.90	0.38	0.64	0.27	0.57	0.50
r203	895.54[d]	895.54	0.00	5.88	2.31	3.35	1.32	2.39	0.94	1.61	0.54	1.09	0.36	0.20	0.00
r204	780.91[b]	780.91	0.00	5.35	4.26	3.59	2.41	2.55	1.71	1.72	0.97	1.15	0.65	1.03	0.13
r205	987.22[b]	987.22	0.00	2.37	2.31	1.39	1.36	1.01	0.99	0.70	0.58	0.48	0.40	0.43	0.00
r206	922.70[d]	922.70	0.00	5.80	3.16	3.39	1.85	2.45	1.34	1.68	0.78	1.15	0.54	0.60	0.00
r207	843.20[c]	857.07	1.64	3.60	2.60	2.11	1.92	1.93	1.80	2.09	**1.55**	1.72	**1.24**	1.69	**1.01**
r208	736.12[d]	738.84	0.37	2.84	2.34	2.05	1.97	1.89	1.56	1.61	1.32	1.42	1.22	1.06	0.80
r209	863.36[c]	870.68	0.85	3.86	2.31	2.23	2.18	1.60	1.13	1.89	1.07	1.74	1.05	1.28	0.93
r210	843.36[d]	846.62	0.39	3.69	2.09	2.09	1.57	1.89	1.40	1.63	1.02	1.51	0.85	1.05	0.68
r211	826.88[c]	826.88	0.00	5.98	3.05	3.46	1.76	2.49	1.27	1.70	0.73	1.16	0.50	1.04	0.00
rc101	1648.99[d]	1661.53	0.76	3.87	2.52	2.15	1.89	1.51	1.20	1.00	0.91	0.96	**0.57**	0.83	**0.32**
rc102	1510.16[c]	1510.16	0.00	4.08	3.09	3.68	1.87	2.72	1.38	1.92	0.84	1.35	0.59	0.90	0.00
rc103	1346.83[b]	1346.83	0.00	1.87	1.11	1.06	0.63	0.76	0.45	0.51	0.26	0.34	0.17	0.31	0.28
rc104	1175.06[c]	1175.83	0.07	4.37	1.96	2.67	1.20	1.98	0.89	1.40	0.54	0.99	0.38	0.90	0.46

rc105	1446.30[b]	1446.30	0.00	4.39	2.98	2.50	1.70	1.78	1.21	1.20	0.69	0.81	0.46	0.72	0.00
rc106	1383.14[b]	1383.14	0.00	6.65	4.91	3.98	2.94	2.92	2.16	2.04	1.29	1.42	0.90	0.20	0.00
rc107	1244.83[b]	1244.83	0.00	6.98	4.13	4.00	2.37	2.86	1.69	1.94	0.97	1.31	0.66	0.50	0.15
rc108	1154.14[c]	1159.90	0.50	4.66	3.41	2.74	2.01	2.00	1.46	1.38	0.86	0.95	0.59	0.86	0.62
rc201	1443.07[b]	1443.07	0.00	2.33	1.13	1.36	0.66	0.98	0.47	0.67	0.28	0.46	0.19	0.41	0.04
rc202	1403.32[b]	1403.32	0.00	3.50	1.96	1.97	1.10	1.39	0.78	0.93	0.44	0.62	0.29	0.56	0.00
rc203	1060.32[c]	1068.28	0.75	4.47	2.29	3.72	1.99	3.02	1.73	2.52	1.20	1.92	0.84	1.58	**0.58**
rc204	884.75[c]	884.97	0.02	3.49	2.71	2.93	1.96	2.16	1.68	1.77	1.05	1.52	0.76	1.09	0.43
rc205	1249.56[b]	1249.56	0.00	4.27	3.02	2.60	1.84	1.94	1.37	1.37	0.84	0.97	0.59	0.88	0.39
rc206	1187.40[b]	1187.40	0.00	3.65	2.02	2.08	1.15	1.48	0.82	1.00	0.47	0.67	0.32	0.60	0.08
rc207	985.67[c]	996.63	1.11	4.97	3.32	2.90	2.24	2.10	1.90	1.94	1.66	2.02	1.32	1.78	**0.86**
rc208	833.12[c]	833.12	0.00	4.79	3.08	2.82	1.81	2.05	1.32	1.42	0.78	0.98	0.54	0.88	0.21
Avg	*1247.77*	*1043.39*	*0.14*	*4.55*	*2.66*	*2.80*	*1.63*	*2.06*	*1.20*	*1.48*	*0.76*	*1.07*	*0.54*	*0.68*	*0.20*

[a] Results of Cortés-Murcia et al.(2019), programmed in C++ and executed on 2.3 GHz Intel Xeon with 8 GB RAM

[b] Best-known solution provided by Cortés-Murcia et al.(2019)

[c] Best-known solution provided by Hiermann et al.(2019)

[d] Best-known solution provided by Keskin and Çatay (2016)

From the results in Table 6, we can see that applying the traditional TA ("C1") cannot provide better results. The average gap between the best (average) solutions and the best-known solutions equals 2.66% (4.55%). After applying the multi-start approach, we can observe that the solutions' quality has improved compared to the traditional TA, with an average gap of 1.03% (1.75%) (between C2 and C1). This improvement is due to the diversification SA mechanism to explore different search regions. In addition, a clear improvement is obtained using the shaking phase in the TA (C3), with an average gap of 1.46% (2.49%) compared to C1. Thus, configurations C2 and C3 show that using our multi-start and shaking phase contributes positively to the quality of solutions and outperforms the traditional TA. However, it still lacks intensification capabilities to improve the solutions, which the intensification case is clearly shown in C4. Using the updating neighborhood search into the shaking phase (C4) is beneficial to enhance the performance of the TA by obtaining an improvement in the instance r207 (in bold) compared to the one obtained by Cortés-Murcia et al. (2019). Comparing configurations C3 and C4, updating the neighborhood search into the shaking phase can improve the quality of the solution with an average of 0.44% (0.99%) (between C3 and C4). This can be explained by the good intensification capabilities of this procedure (C4) compared to the traditional technique in the shaking phase (C3), which is consistent with the work of Karakostas and Sifalera (2022). One of the main interesting points for applying both multi-start and shaking phase (without updating neighborhood search), as shown in C5, permits better space exploration and improves the efficiency of using them in different combinations separately. With an average gap between C5 and C3 of the best runs (column Best%) is equal to 0.66% (1.20% - 0.54%) and 0.99% (2.06% - 1.07%) for the five runs (column Avg%). For the case of C5 and C4, the average gap of the best runs is 0.22% (0.76% - 0.54%) and 0.41% (1.48% - 1.07%) for five runs. Moreover, we can observe that applying these two components can improve the quality of the solution, where three instances (indicated in bold) are better than in Cortés-Murcia et al. (2019). However, the average gap in this configuration is still high compared to that found by the hybrid ILS of Cortés-Murcia et al. (2019). As a result, when applying both all diversification and intensification mechanisms of the multi-start, shaking phase and updating the neighborhood search (C6) give good results by providing five better solutions compared to Cortés-Murcia et al. (2019) even with a small high average (column Best%) of 0.20% compared to 0.14% of the hybrid ILS. In conclusion, applying all new components to the traditional TA provides the most effective configuration.

6.3. Analysis on the HWCP instances

We present the results on the small- and large-sized instances in Figures 2 and 3, respectively. In Figure 2.a, we provide the percentage deviation from the best solution ("Best") found after 10 minutes for the small instances, and after 20 minutes for large-sized instances in Figure 3.a. Figures 2.b and 3.b present the percentage of deviation from the best results solution obtained in terms of kilometers driven with each fuel type (electricity and CNG), found after 10 minutes for the small instances and after 20 minutes for large-sized instances. Each instance of each data set (C, R, and RC) is run five times. For all small instances with up 20 customers, each instance was solved in 10 minutes by the proposed hybrid algorithm. The average of five runs after 2, 3, 4, 5, and 6 minutes, and the best solution of each run is compared to the best solution found after 10 minutes. For large-sized instances with up 100 to customers, the best solutions obtained after 10, 12, 14, 16, and 18 minutes are stored, and the best solution values are compared to the best solution found after 20 minutes. The detailed results of these comparisons can be found on the previously mentioned website.

(a) Best and averages results solutions (deviation with respect to 10 min runtime)

(b) Km driven with each fuel type (deviation with respect to 10 min runtime)
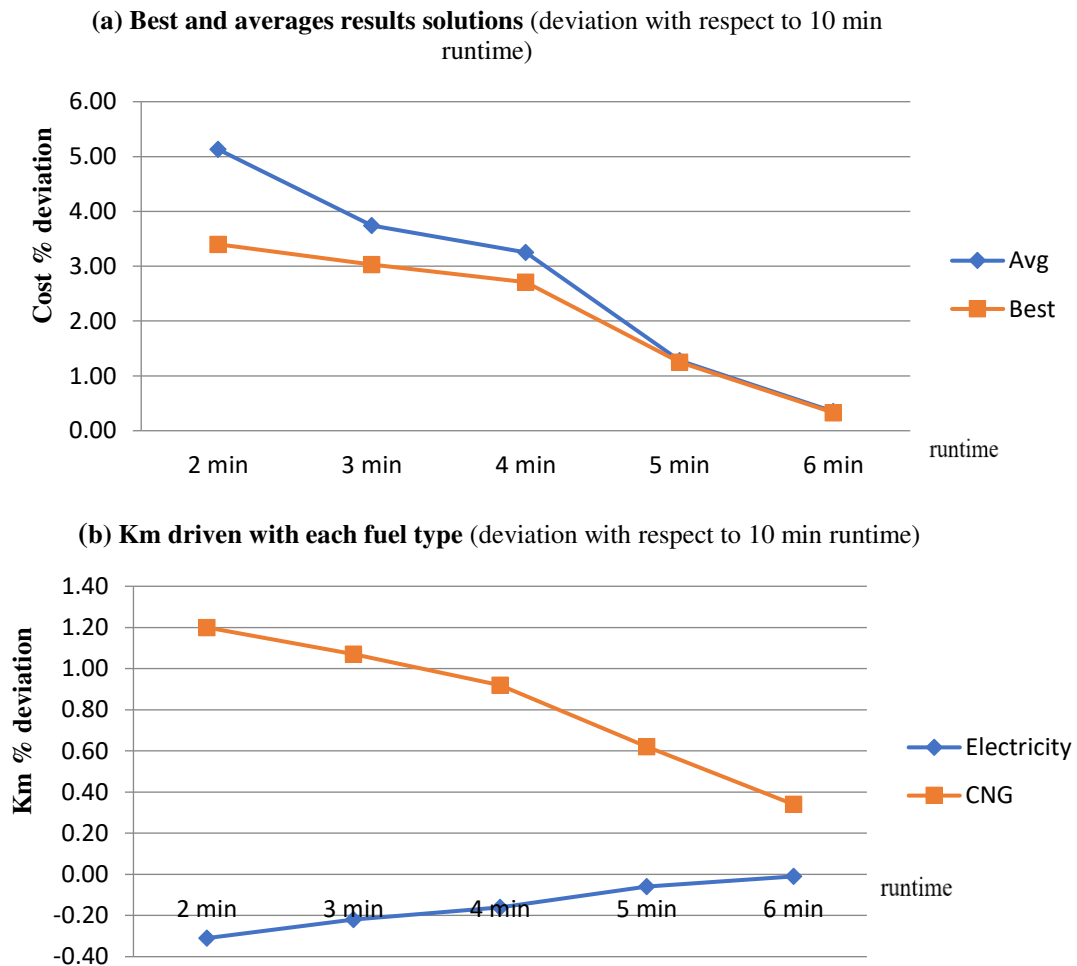
Figure 2: Results for small-sized instances

Figure 2.a shows that, on average, solutions found after two minutes deviate 3.40% from the best solution found in 10 minutes. A decrease of 0.37% (3.40% - 3.03%) occurs when the limited time varies from two to three minutes. Furthermore, a decrease in change of the gaps with as well as a 0.32% (3.03% - 2.71%) for the case when the limited time changes from three to four minutes, and 2.38% (2.71% - 0.33%) for the case when the run time changes from four to six minutes. After six minutes of running time, this difference is reduced to

24

0.33%. The improvement and the shape of the solution are related to reducing the traveled distance using CNG fuel and increasing the use of electric energy over time, as shown in Figure 2.b. In other words, the difference in the total traveled distance using CNG is decreased from 1,20% (in 2 minutes) to 0.34% (in 6 minutes) while an increase from -0.31% (in 2 minutes) to -0.01% (in 6 minutes) in terms of total distance using electricity is observed when compared to the solutions obtained after 10 minutes. Observing the number of visits to landfills, electricity, and CNG recharging stations, we can see that the same number of stations is visited over time. Thus, we can conclude that the consumption of energy/CNG during the route impacts the quality of solutions and their total cost.

(a) Best and averages results solutions (deviation with respect to 20 min runtime)

(b) Km driven with each fuel type (deviation with respect to 20 min runtime)
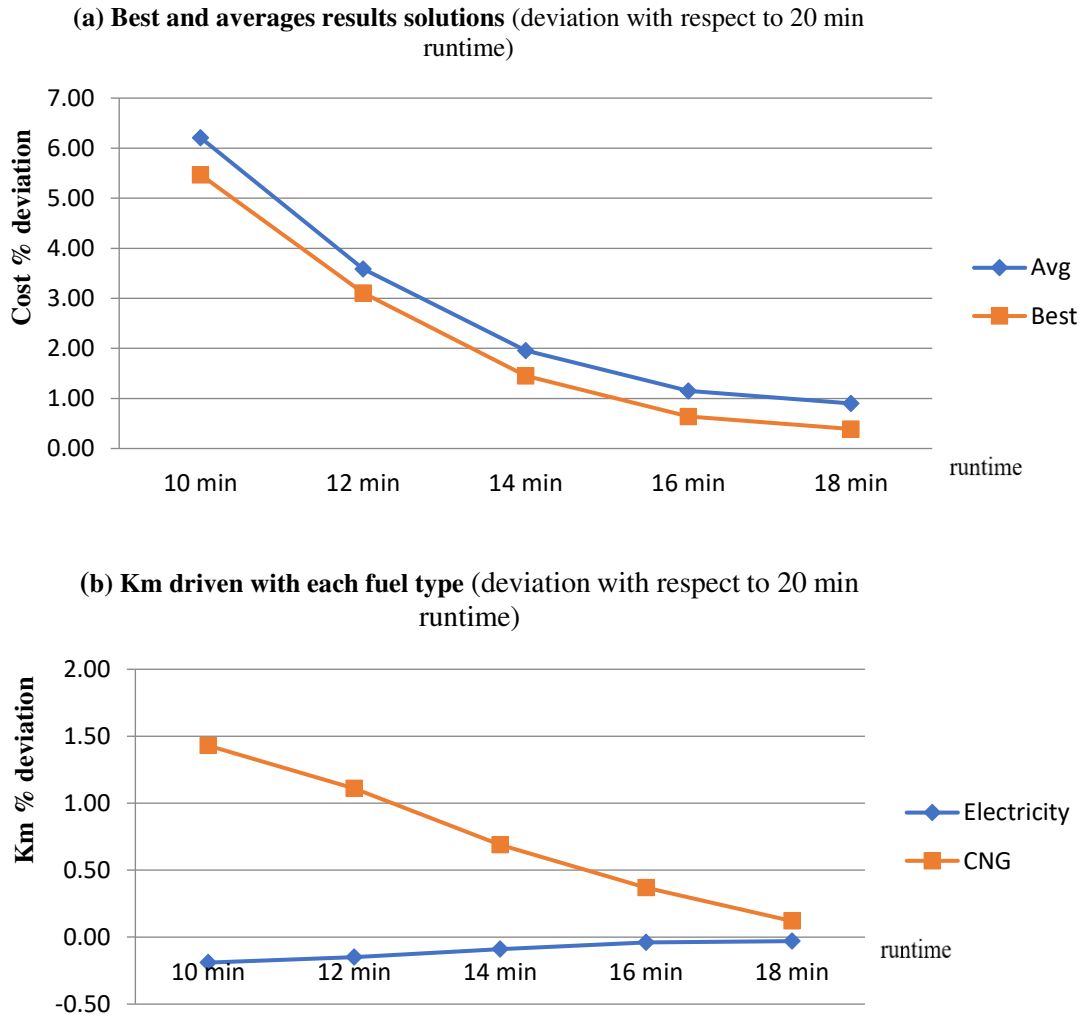
Figure 3: Results for large-sized instances

In Figure 3.a, we can observe that the gap to the solution cost obtained after 20 minutes is about 6% for a 10-minute runtime and that this gap is decreased by half for every 2 min added to the runtime. One of the most interesting observations from these results is that, unlike the tests on the small instances, the additional number of electric and CNG stations impacts the planning of routes and the quality of solutions over time. Based on the detailed results (available online), in 12 out of 20 instances, the number of CNG (electric) stations visited when the runtime is 10 minutes is larger than when the runtime is 20 minutes. Similar observations can be found for the different times, i.e., 12, 14, 16 minutes. The number of refueling visits is similar in 18 and 20

min, but with different distances traveled. This may be due to the slight difference in the recharging/refueling nodes used.

As we obtained managerial insight from these instances, the most significant improvement is based on the consumption of each fuel type along the trip. In Figure 3.b, the total deviation of the traveled distance using CNG is decreased from 1.43% (in 10 minutes) to 0.12% (in 18 minutes), while it increases from 0.03% to 0.19% in terms of total traveled distance using electricity.

Figures 2 and 3 show that the objective function values converge with the increase in computational times. This articulates that our algorithm's diversification and intensification mechanisms considerably improve the solution quality over time.

Figure 4 depicts the improvement percentage of the HTA over the first ten minutes for the large size instance. In all experiments, we use the average gap to the best solution. This paper selects two instances from each data set C, R, RC with different time windows and number of customers to show the convergence curves of the solution over time.
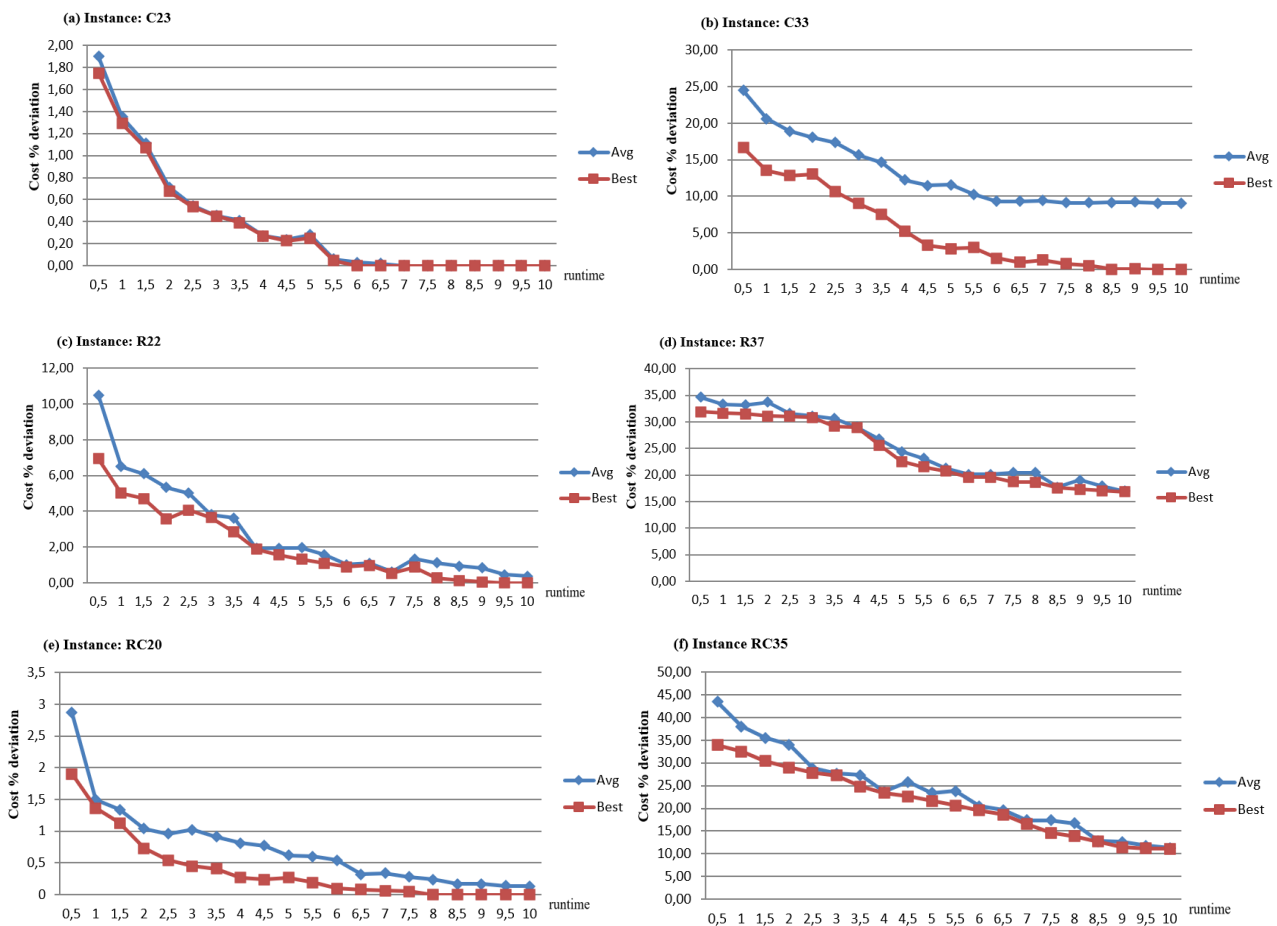
Figure 4: Convergence curve of the HTA during the first ten minutes

Looking at Figure 4, we can see that the HTA converges slowly but achieves excellent solutions, a trade-off often seen in metaheuristics (Talbi, 2009). This is because our procedure balances exploitation and global exploration to avoid the problem of converging too quickly to a non-acceptable local optimum. In addition, we can observe from Figure 4.a that in the instance C23, the algorithm converges and obtains the best solution after only around 6 minutes.

6.4. Impact of using compressed natural gas plug-in hybrid electric vehicles

We now investigate the impact of using CNG-PHEVs compared to pure CNG and pure EVs. The CNG-PHEVs use two fuel types, while CNG vehicles may only use CNG, and the EV uses only electricity. Both vehicles can recharge (refuel) their battery (tank) from an external station. We consider different battery and tank capacities to assess their impact on the use of recharging/refueling stations in terms of traversed distance and solution quality. We consider that each capacity (tank and battery) is multiplied by 1.5 and 2.0 in our experiments. In other words, if the regular battery capacity value is equal to 40 KW, we also test parameters 60 KW and 80KW, and likewise for the tank capacity. To this end, different battery and fuel tank capacities are considered. Table 7 summarizes all these different configuration values. For example, in configuration R2, the CNG-PHEV fleet contains regular tanks and 1.5 the battery values.

Table 7
Different configuration tank and battery capacities

| Configuration	Description
R1	regular tank and regular battery (main values)
R2	regular tank and 1.5 regular battery
R3	regular tank and 2.0 regular battery
R4	1.5 regular tank and regular battery
R5	2.0 regular tank and regular battery
R6	2.0 regular tank and 1.5 regular battery
R7	1.5 regular tank and 1.5 regular battery
R8	1.5 regular tank and 2.0 regular battery

Figure 5 shows the results of the different comparisons on a small set of instances with different characteristics, such as tight and wide time windows, number of landfills, and randomly/clustered landfill locations. Figure 5.a shows the comparison between the different CNG-PHEV configurations (R2-R8) against the regular CNG-PHEVs fleet (R1). For each configuration, we compare the obtained results in terms of distance and cost for each configuration R2-R8 with the one obtained by R1.

(a) Comparison of different CNG-PHEV configurations
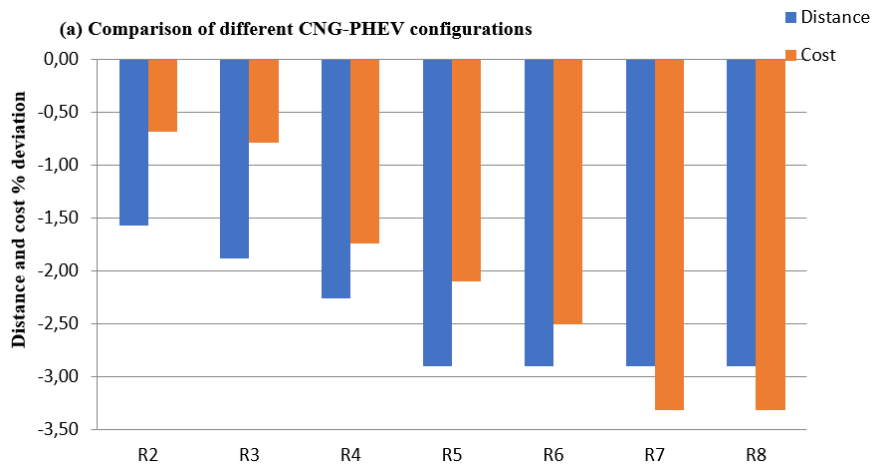
.The detailed results in Figure 5.a highlight that using a fleet of CNG-PHEVs with increased capacity values decreases the total traveling distance and costs for all different configurations. Using a doubled battery or tank capacity (configurations R3, R5, R6, and R8) yields the same distance reduction of almost 3% with

respect to the regular capacities R1. Indeed, the detailed solutions show that using a double-sized battery or tank is sufficient to serve all customers with fewer visits to recharging/refueling stations compared to the regular R1. In addition, using a double battery capacity leads to the best cost reduction observed in configurations R3 and R8, with an average improvement of 3.38% compared to the costs of configuration R1. Moreover, configurations R3 and R8 provide the best total traveled distance and costs compared to other configurations. In general, we can observe that increasing the battery capacity significantly impacts the number of recharging stations visited.

We also assess the performance of different fleets. Figures 5.b and 5.c compare pure CNG vehicles and pure EVs with different tank and battery capacities against regular CNG-PHEVs (R1).
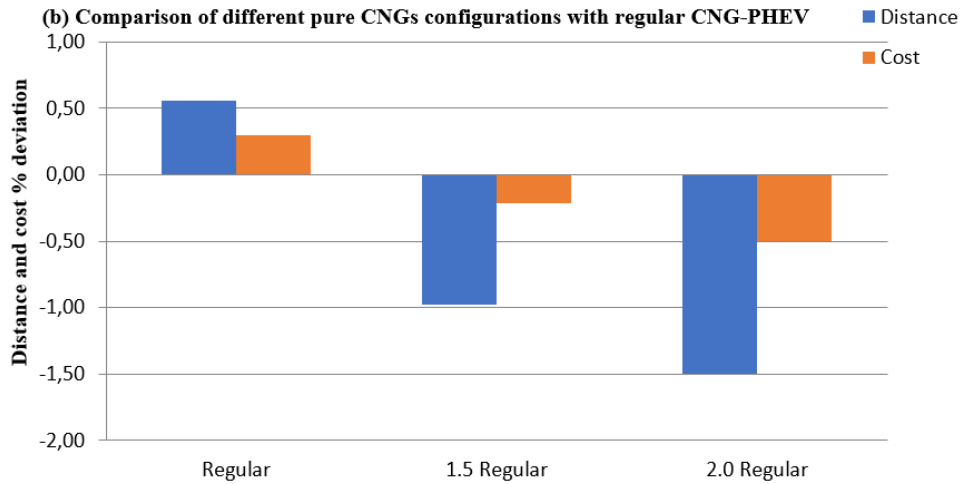
The detailed results of Figure 5.b show that using a fleet of CNG vehicles with a regular tank capacity leads to an increase in the distance and cost of the solution compared to configuration R1 containing a hybrid fleet. An increased tank capacity decreases the total traveling distance (costs) with an average gap equal to 1.01% (0.22%) for the CNG vehicles with 1.5 times the regular tank capacity tank, and by 1.54% (0.51%) when using 2.0 times the regular capacity values.
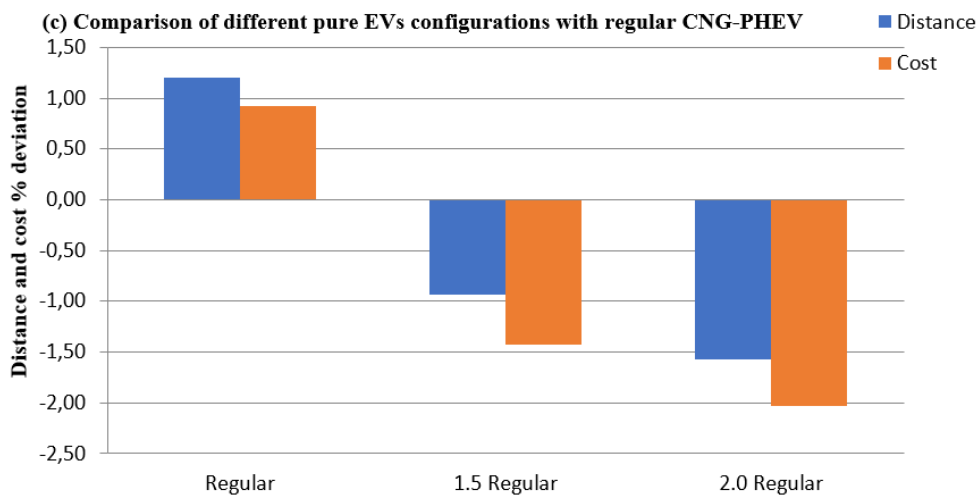

Figure 5: Impact of the battery and tank capacities

Similar observations can be made when using pure EVs in Figure 5.c when using a larger battery capacity that decreases the total traveled distance and cost. As in the case of pure CNGs, a fleet of pure EVs with larger batteries can serve the customers and visit the landfills with fewer visits to recharging stations. The total

traveled distance and costs are increased by 1.23% and 0.94%, respectively, when using a regular battery compared to the original fleet in configuration R1. This is due to additional distances to visit the recharging stations.

Finally, we also investigate the impact of adopting a realistic fuel consumption function in our HTA. To this end, we have applied two different strategies: a realistic consumption function (strategy 1 as used in this paper) and constant consumption (strategy 2), which uses a constant rate equal to 380 W/mile (EPA, 2016) and a constant CNG consumption rate that is equal to 0.19 diesel gallon/mile (ampCNG, 2015).

Table 8 provides the obtained results for the energy and CNG consumption fuels for each strategy. Column % presents the percentage deviations from the best (average) solution obtained by our algorithm using the first strategy by comparing the electricity consumption (CNG consumption) found in strategy 2 to the energy consumption obtained by strategy 1. We note that in the detailed results of this table on the website, the Column "Nb-CNG (Nb-Elec)" shows the available number of CNG (electric) stations in each instance. In Column "Nb-fuel", we present the number of recharging/refueling performed by the vehicles.

Table 8

The comparison between the two strategies

Dataset	HTA with strategy 1 (realistic)				HTA with strategy 2 (constant rate)							
	Best		Avg		Best				Avg			
	Electric	CNG	Electric	CNG	Electric	%	CNG	%	Electric	%	CNG	%
C	769.04	431.51	802.57	441.02	799.73	4.09	458.88	6.34	800.03	4.13	466.10	8.01
R	804.02	431.98	821.58	441.21	838.56	4.31	459.75	6.43	838.92	4.36	466.55	8.00
RC	785.06	432.07	803.35	441.86	822.66	4.95	459.53	6.36	822.99	4.99	465.52	7.75
Avg	*786.04*	*431.85*	*809.17*	*441.36*	*820.31*	*4.45*	*459.39*	*6.38*	*820.64*	*4.49*	*466.06*	*7.92*

As seen from the table, the realistic consumption instances (strategy 1) perform better than the second strategy in terms of electric consumption and CNG fuel. The average gap to the best electricity consumption is equal to 4.45% and ranges between 0.10% and 13.33%, while the average gap to the best CNG consumption is equal to 6.38% and ranges between 3.38% and 9.22%. Compared to the first strategy for the total consumed electricity (column Avg), the average deviation from the result solutions is 4.49% for the electric consumption and 7.92% for the CNG fuel. These results show that integrating the impact of different factors (aerodynamic drag, load, vehicle speed, acceleration, etc.) affects the energy consumption, leading to less fuel consumption, rather than considering a constant consumption value which has been confirmed by Masmoudi et al. (2018b), and Macrina et al. (2019).

Based on the above experimental results, managerial insights can be suggested for industry and can be applied in real-life applications:

i) The logistics industry has a crucial role in supply chain and transportation. The investigated HWCP can be used to improve a company's operations in charge of collecting waste by reducing their total travel costs. This study opens a discussion for a new problem, the WCVRP, which studies a new fleet of CNG-PHEVs by obtaining the most efficient routes to visit the most bins within a certain time limit. Results highlight the profitable use and a general application of CNG-PHEVs. The studied problem is quite complex as it simultaneously deals with route optimization and recharging-refueling decisions and considers a complex network with intersection nodes.

ii) Our analyses highlight that government and industry should invest more to increase the number of CNG-PHEVs due to the environmental benefits and ability to use two alternative fuels (CNG and electricity) in the same vehicle. The developed HTA is proven to be a powerful tool in terms of efficiency and effectiveness in exploiting this flexibility.

iii) Also, this research invites companies to replace their conventional vehicles (with diesel/gasoline fuel) or with traditional HEV (two fuel sources; electric and diesel fuel) with CNG-PHEV due to their advantages of low energy consumption, low pollution and GHG emissions since two alternative fuels can be used.

iv) CNG-PHEV can be a temporary solution in electrification because they satisfy emission regulations without sacrificing the driving range. The use of EVs can cause drivers anxiety due to low battery capacities. However, CNG-PHEVs ensure regulations are respected without any range anxiety issues.

v) Moreover, using CNG-PHEVs can provide lower costs than using a fleet of pure CNGs or EVs. In addition, it is preferable for the industry to use larger batteries, as demonstrated in our detailed experimental results, due to their benefit in terms of total costs.

7. Conclusions

We have studied the Waste Collection Vehicle Routing Problem with Time Windows (WCVRPTW) using a fleet of Compressed Natural Gas Plug-in Hybrid Electric Vehicles (CNG-PHEVs). This variant is denoted as the Hybrid Waste Collection Problem (HWCP). Hybrid vehicles introduce the challenge of planning routes for vehicles with two different power sources. Moreover, we utilize a realistic fuel consumption model that considers various features such as the road gradient and the path between two customer nodes, which allows the detailed calculation of the fuel and energy required during the trip besides allowing refueling/recharging of CNG-PHEVs. The problem is highly complex as it simultaneously considers route optimization and recharging-refueling decisions. An advanced solution method is developed to ensure that CNG-PHEV can be used in practice. Our Hybrid Threshold Acceptance (HTA) algorithm is guided by an efficient constructive heuristic, a diversification mechanism based on a multi-start approach, and an advanced deterministic and shaking procedure for the intensification mechanism. Extensive numerical experiments show that our HTA provides good solutions to the new HWCP instances and the EVRP(-PR) benchmark instances. The proposed HTA algorithm provides good results against state-of-the-art algorithms, particularly the hybrid GA of Hiermann et al. (2019) on the EVRP instances with full recharging and with the ILS of Cortés-Murcia et al. (2019).

Sensitivity analyses have been conducted to study the impact and effect of the CNG-PHEVs on operational costs and traveling distances. A comparison between electric and CNG vehicles has also been provided. It is shown that using a fleet of CNG-PHEVs is beneficial and offers a good trade-off between operational costs and distances traveled, compared to using only electric or CNG vehicles. Optimized solutions for the HWCP can help companies or organizations reduce their total traveling costs by obtaining improved routing solutions while reaching consumers on time. In addition, computational experiments illustrated that stakeholders should focus on increasing the number of charging stations to reduce the dependency on fossil-based fuels. This

research also highlights the importance of replacing conventional vehicles with fuel-efficient vehicles as well as environmentally friendly ones.

We aim to study a more practical variant in future work, namely the multi-depot WCVRPTW with synchronization constraints and a mixed fleet of electric vehicles.

Acknowledgments

References

Abid, M., & Tabaa, M. (2022). Routing and Charging of Electric Vehicles: Survey. In *Advances on Smart and Soft Computing* (pp. 211-223). Springer, Singapore.

Advantage Environnment (2011). The world's first hybrid garbage truck. URL: http://advantage environment.com/transport/the-worlds-first-hybrid-garbage-truck/

Airuse (2016). Strategies to encourage use of electric, hybrid electric and gas vehicles in Northern and Central Europe.

ampCNG (2015). The per-mile Costs of Operating Compressed Natural Gas Trucks.

Arslan, O., Yıldız, B., & Karaşan, O. E. (2015). Minimum cost path problem for plug-in hybrid electric vehicles. *Transportation Research Part E: Logistics and Transportation Review*, *80*, 123-141.

Asghari, M., & Al-e, S. M. J. M. (2020). Green vehicle routing problem: A state-of-the-art review. *International Journal of Production Economics*, 107899.

Bahrami, S., Nourinejad, M., Amirjamshidi, G., & Roorda, M. J. (2020). The Plugin Hybrid Electric Vehicle routing problem: A power-management strategy model. *Transportation Research Part C: Emerging Technologies*, *111*, 318-333.

Barth, M., & Boriboonsomsin, K. (2009). Energy and emissions impacts of a freeway-based dynamic eco-driving system. *Transportation Research Part D: Transport and Environment*, *14*(6), 400-410.

Basso, R., Kulcsár, B., Sanchez-Diaz, I., & Qu, X. (2022). Dynamic stochastic electric vehicle routing with safe reinforcement learning. *Transportation research part E: logistics and transportation review*, *157*, 102496.

Bautista, J., Fernández, E., & Pereira, J. (2008). Solving an urban waste collection problem using ants heuristics. *Computers & Operations Research*, *35*(9), 3020-3033.

Beek, O., Raa, B., Dullaert, W., & Vigo, D. (2018). An efficient implementation of a static move descriptor-based local search heuristic. *Computers & Operations Research*, *94*, 1-10.

Bektaş, T., & Laporte, G. (2011). The pollution-routing problem. *Transportation Research Part B: Methodological*, *45*(8), 1232-1250.

Bektaş, T., Ehmke, J. F., Psaraftis, H. N., & Puchinger, J. (2019). The role of operational research in green freight transportation. *European Journal of Operational Research*, *274*(3), 807-823.

Benjamin, A. M., & Beasley, J. E. (2010). Metaheuristics for the waste collection vehicle routing problem with time windows, driver rest period and multiple disposal facilities. *Computers & Operations Research*, *37*(12), 2270-2280.

Braekers, K., Caris, A., & Janssens, G. K. (2014). Exact and meta-heuristic approach for a general heterogeneous dial-a-ride problem with multiple depots. *Transportation Research Part B: Methodological*, *67*, 166-186.

Bräysy, O., Dullaert, W., Hasle, G., Mester, D., & Gendreau, M. (2008). An effective multirestart deterministic annealing metaheuristic for the fleet size and mix vehicle-routing problem with time windows. *Transportation Science*, *42*(3), 371-386.

Chen, H., He, J., & Zhong, X. (2019). Engine combustion and emission fuelled with natural gas: a review. *Journal of the Energy Institute*, *92*(4), 1123-1136

Cortés-Murcia, D. L., Prodhon, C., & Afsar, H. M. (2019). The electric vehicle routing problem with time windows, partial recharges and satellite customers. *Transportation Research Part E: Logistics and Transportation Review*, *130*, 184-206.

Das, S., & Bhattacharyya, B. K. (2015). Optimization of municipal solid waste collection and transportation routes. *Waste Management*, *43*, 9-18.

Demir, E., Bektaş, T., & Laporte, G. (2011). A comparative analysis of several vehicle emission models for road freight transportation. *Transportation Research Part D: Transport and Environment*, *16*(5), 347-357.

Demir, E., Bektaş, T., & Laporte, G. (2012). An adaptive large neighborhood search heuristic for the pollution-routing problem. *European Journal of Operational Research*, *223*(2), 346-359.

Demir, E., Bektaş, T., & Laporte, G. (2014). A review of recent research on green road freight transportation. *European Journal of Operational Research*, *237*(3), 775-793.

Demir, E., Huang, Y., Scholts, S., & Van Woensel, T. (2015). A selected review on the negative externalities of the freight transportation: Modeling and pricing. *Transportation Research Part E: Logistics and Transportation Review*, *77*, 95-114.

Dongarra, J. (2014). Performance of Various Computers Using Standard Linear Equations Software, (Linpack Benchmark Technical Report, CS-89-85). University of Tennessee, Computer Science

EPA (2016). The EPA 10 gallon per minute fuel dispensing limit U. E. P. agency. 40 CFR 80.22.

EPA, (2012). Motor vehicle emission simulator (MOVES): User's guide for MOVES2010b. Technical report, United States Environmental Protection Agency, USA.

Ercan, T., Zhao, Y., Tatari, O., & Pazour, J. A. (2015). Optimization of transit bus fleet's life cycle assessment impacts with alternative fuel options. *Energy*, *93*, 323-334.

Erdoğan, S., & Miller-Hooks, E. (2012). A green vehicle routing problem. *Transportation Research Part E: Logistics and Transportation Review*, *48*(1), 100-114.

Eurostat (2017): Municipal Waste Statistics. URL: https://ec.europa.eu/eurostat/statistics explained/index.php/

Goeke, D., & Schneider, M. (2015). Routing a mixed fleet of electric and conventional vehicles. *European Journal of Operational Research*, *245*(1), 81-99.

Golden BL, Assad AA, Wasil EA. Routing vehicles in the real world: applications in the solid waste, beverage, food, dairy, and newspaper industries. In: Toth P, Vigo D, editors. The Vehicle Routing Problem. Philadelphia, PA: SIAM; 2002.

Green Fleet (2008). The World's First CNG-Powered Plug-In Hybrid Refuse Vehicle Hits the Pavement.

Hagos, F. Y., Aziz, A. R. A., Sulaiman, S. A., & Mahgoub, B. K. (2016). Low and medium calorific value gasification gas combustion in IC engines. In *Developments in Combustion Technology*. IntechOpen.

Han, H., & Ponce Cueto, E. (2015). Waste collection vehicle routing problem: literature review. *PROMET-Traffic&Transportation*, *27*(4), 345-358.

Hannan, M. A., Akhtar, M., Begum, R. A., Basri, H., Hussain, A., & Scavino, E. (2018). Capacitated vehicle-routing problem model for scheduled solid waste collection and route optimization using PSO algorithm. *Waste Management*, *71*, 31-41.

Hemmelmayr, V. C., Doerner, K. F., & Hartl, R. F. (2009). A variable neighborhood search heuristic for periodic routing problems. *European Journal of Operational Research*, *195*(3), 791-802.

Heni, H., Arona Diop, S., Renaud, J., & Coelho, L. C. (2021). Measuring fuel consumption in vehicle routing: new estimation models using supervised learning. *International Journal of Production Research*, 1-17.

Heni, H., Coelho, L. C., & Renaud, J. (2019). Determining time-dependent minimum cost paths under several objectives. *Computers & Operations Research*, *105*, 102-117.

Hiermann, G., Hartl, R. F., Puchinger, J., & Vidal, T. (2019). Routing a mix of conventional, plug-in hybrid, and electric vehicles. *European Journal of Operational Research*, *272*(1), 235-248.

HVT (2012). Hybrid Vehicle Timeline. Available on the URL http://www.hybridcenter.org/hybrid-timeline.html

Jaballah, R., Veenstra, M., Coelho, L. C., & Renaud, J. (2021). The time-dependent shortest path and vehicle routing problem. *INFOR: Information Systems and Operational Research*, *59*(4), 592-622.

Karadimas, N. V., Papatzelou, K., & Loumos, V. G. (2007, September). Genetic algorithms for municipal solid waste collection and routing optimization. In *IFIP International Conference on Artificial Intelligence Applications and Innovations* (pp. 223-231). Springer, Boston, MA.

Keskin, M., & Çatay, B. (2016). Partial recharge strategies for the electric vehicle routing problem with time windows. *Transportation research part C: emerging technologies*, *65*, 111-127.

Kim, B. I., Kim, S., & Sahoo, S. (2006). Waste collection vehicle routing problem with time windows. *Computers & Operations Research*, *33*(12), 3624-3642.

Koç, Ç., Jabali, O., Mendoza, J. E., & Laporte, G. (2019). The electric vehicle routing problem with shared charging stations. *International Transactions in Operational Research*, *26*(4), 1211-1243.

Kucukoglu, I., Dewil, R., & Cattrysse, D. (2021). The electric vehicle routing problem and its variations: A literature review. *Computers & Industrial Engineering*, *161*, 107650.

Lee, C. K. M., Yeung, C. L., Xiong, Z. R., & Chung, S. H. (2016). A mathematical model for municipal solid waste management–A case study in Hong Kong. *Waste Management*, *58*, 430-441.

Leung, S. C., Zhang, Z., Zhang, D., Hua, X., & Lim, M. K. (2013). A meta-heuristic algorithm for heterogeneous fleet vehicle routing problems with two-dimensional loading constraints. *European Journal of Operational Research*, *225*(2), 199-210.

Lin, D. Y., & Kuo, J. K. (2021). The vehicle deployment and relocation problem for electric vehicle sharing systems considering demand and parking space stochasticity. *Transportation Research Part E: Logistics and Transportation Review*, *156*, 102514.

Lin, S. (1965). Computer solutions of the traveling salesman problem. *Bell System Technical Journal*, *44*(10), 2245-2269.

Liu, J., & He, Y. (2012). A clustering-based multiple ant colony system for the waste collection vehicle routing problems. In *2012 Fifth International Symposium on Computational Intelligence and Design* (Vol. 2, pp. 182-185). IEEE.

Liu, S., Huang, W., & Ma, H. (2009). An effective genetic algorithm for the fleet size and mix vehicle routing problems. *Transportation Research Part E: Logistics and Transportation Review*, *45*(3), 434-445.

Linpack (2016). Available on http://www.roylongbottom.org.uk/. Last accessed on 15/06/2022.

Louati, A. (2016). Modeling municipal solid waste collection: A generalized vehicle routing model with multiple transfer stations, gather sites and inhomogeneous vehicles in time windows. *Waste Management*, *52*, 34-49.

Lu, C. C., Diabat, A., Li, Y. T., & Yang, Y. M. (2022). Combined passenger and parcel transportation using a mixed fleet of electric and gasoline vehicles. *Transportation Research Part E: Logistics and Transportation Review*, *157*, 102546.

Macrina, G., Laporte, G., Guerriero, F., & Pugliese, L. D. P. (2019). An energy-efficient green-vehicle routing problem with mixed vehicle fleet, partial battery recharging and time windows. *European Journal of Operational Research*, *276*(3), 971-982.

Mancini, S. (2017). The hybrid vehicle routing problem. *Transportation Research Part C: Emerging Technologies*, *78*, 1-12.

Masmoudi, M. A., Braekers, K., Masmoudi, M., & Dammak, A. (2017). A hybrid genetic algorithm for the heterogeneous dial-a-ride problem. *Computers & Operations Research*, *81*, 1-13.

Masmoudi, M. A., Hosny, M., Braekers, K., & Dammak, A. (2016). Three effective metaheuristics to solve the multi-depot multi-trip heterogeneous dial-a-ride problem. *Transportation Research Part E: Logistics and Transportation Review*, *96*, 60-80.

Masmoudi, M. A., Hosny, M., Demir, E., & Cheikhrouhou, N. (2018a). A study on the heterogeneous fleet of alternative fuel vehicles: Reducing CO2 emissions by means of biodiesel fuel. *Transportation Research Part D: Transport and Environment*, *63*, 137-155.

Masmoudi, M. A., Hosny, M., Demir, E., & Pesch, E. (2020). Hybrid adaptive large neighborhood search algorithm for the mixed fleet heterogeneous dial-a-ride problem. *Journal of Heuristics*, *26*(1), 83-118.

Masmoudi, M. A., Hosny, M., Demir, E., Genikomsakis, K. N., & Cheikhrouhou, N. (2018b). The dial-a-ride problem with electric vehicles and battery swapping stations. *Transportation Research Part E: Logistics and Transportation Review*, *118*, 392-420.

Mesjasz-Lech, A., & Michelberger, P. (2019). Sustainable Waste Logistics and the Development of Trade in Recyclable Raw Materials in Poland and Hungary. *Sustainability*, *11*(15), 4159.

Mladenović, N., & Hansen, P. (1997). Variable neighborhood search. *Computers & operations research*, *24*(11), 1097-1100.

Montoya, A., Guéret, C., Mendoza, J. E., & Villegas, J. G. (2016). A multi-space sampling heuristic for the green vehicle routing problem. *Transportation Research Part C: Emerging Technologies*, *70*, 113-128.

Municipal_waste_statistics. Last accessed 25/03/2020.

Murakami, K. (2017). A new model and approach to electric and diesel-powered vehicle routing. *Transportation Research Part E: Logistics and Transportation Review*, *107*, 23-37.

Murakami, K. (2018). Formulation and algorithms for route planning problem of plug-in hybrid electric vehicles. *Operational Research*, *18*(2), 497-519.

Nejad, M. M., Mashayekhy, L., Grosu, D., & Chinnam, R. B. (2017). Optimal routing for plug-in hybrid electric vehicles. *Transportation Science*, *51*(4), 1304-1325.

NGC (2017). CNG savings calculator. URL: https://www.cng.co.tt/savings-calculator/.

Nikolakopoulos, A., & Sarimveis, H. (2007). A threshold accepting heuristic with intense local search for the solution of special instances of the traveling salesman problem. *European Journal of Operational Research*, *177*(3), 1911-1929.

Nowakowski, P., Szwarc, K., & Boryczka, U. (2018). Vehicle route planning in e-waste mobile collection on demand supported by artificial intelligence algorithms. *Transportation Research Part D: Transport and Environment*, *63*, 1-22.

Pelletier, S., Jabali, O., Laporte, G., & Veneroni, M. (2017). Battery degradation and behaviour for electric vehicles: Review and numerical analyses of several models. *Transportation Research Part B: Methodological*, *103*, 158-187.

Peng, K., Pan, Q. K., Gao, L., Li, X., Das, S., & Zhang, B. (2019). A multi-start variable neighbourhood descent algorithm for hybrid flowshop rescheduling. *Swarm and Evolutionary Computation*, *45*, 92-112.

Polacek, M., Doerner, K. F., Hartl, R. F., & Maniezzo, V. (2008). A variable neighborhood search for the capacitated arc routing problem with intermediate facilities. *Journal of Heuristics*, *14*(5), 405-423.

Rabbani, M., Heidari, R., Farrokhi-Asl, H., & Rahimi, N. (2018). Using metaheuristic algorithms to solve a multi-objective industrial hazardous waste location-routing problem considering incompatible waste types. *Journal of Cleaner Production*, *170*, 227-241.

Ramos, T. R. P., de Morais, C. S., & Barbosa-Povoa, A. P. (2018). The smart waste collection routing problem: Alternative operational management approaches. *Expert Systems with Applications*, *103*, 146-158.

Renova (2006). Cleanowa-electric-hybrid technology for more environment-friendly waste collection. URL http://ec.europa.eu/environment/life/project/Projects/files/laymanReport/LIFE03_ENV_S_000592_LAYMAN.pdf

Ropke, S., & Pisinger, D. (2006). An adaptive large neighborhood search heuristic for the pickup and delivery problem with time windows. *Transportation Science*, *40*(4), 455-472.

Savelsbergh, M. W. A. (1992). The vehicle routing problem with time windows: Minimizing route duration. *ORSA Journal on Computing*, *4*(2), 146-154.

Schneider, M., Stenger, A., & Goeke, D. (2014). The electric vehicle-routing problem with time windows and recharging stations. *Transportation Science*, *48*(4), 500-520.

Shao, Y., & Dessouky, M. (2020). A routing model and solution approach for alternative fuel vehicles with consideration of the fixed fueling time. *Computers & Industrial Engineering*, *142*, 106364.

Solomon, M. M. (1987). Algorithms for the vehicle routing and scheduling problems with time window constraints. *Operations Research*, *35*(2), 254-265.

Sulemana, A., Donkor, E. A., Forkuo, E. K., & Oduro-Kwarteng, S. (2018). Optimal routing of solid waste collection trucks: a review of methods. *Journal of Engineering*, *2018,* 1-12.

Tahami, H., Rabadi, G., & Haouari, M. (2020). Exact approaches for routing capacitated electric vehicles. *Transportation Research Part E: Logistics and Transportation Review*, *144*, 102126.Lin, D. Y., & Kuo, J. K. (2021). The vehicle deployment and relocation problem for electric vehicle sharing systems considering demand and parking space stochasticity. *Transportation Research Part E: Logistics and Transportation Review*, *156*, 102514.

Talbi, E. G. (2009). *Metaheuristics: From Design to Implementation* (Vol. 74). John Wiley & Sons.

Tirkolaee, E. B., Alinaghian, M., Hosseinabadi, A. A. R., Sasi, M. B., & Sangaiah, A. K. (2019). An improved ant colony optimization for the multi-trip capacitated arc routing problem. *Computers & Electrical Engineering*, *77*, 457-470.

Travesset-Baro, O., Rosas-Casals, M., & Jover, E. (2015). Transport energy consumption in mountainous roads. A comparative case study for internal combustion engines and electric vehicles in Andorra. *Transportation Research Part D: Transport and Environment*, *34*, 16-26.

US DOE, Department of Energy (2011). The Alternative Fuels and Advanced Vehicles Data Center (AFDC). URL: http://www.afdc.energy.gov/afdc/fuels/stations_counts.html. Last accessed 15/06/2022.

Vincent, F. Y., Redi, A. P., Hidayat, Y. A., & Wibowo, O. J. (2017). A simulated annealing heuristic for the hybrid vehicle routing problem. *Applied Soft Computing*, *53*, 119-132.

Vincent, F. Y., & Lin, S. W. (2014). Multi-start simulated annealing heuristic for the location routing problem with simultaneous pickup and delivery. *Applied Soft Computing*, *24*, 284-290.

Vu, H. L., Ng, K. T. W., Fallah, B., Richter, A., & Kabir, G. (2020). Interactions of residential waste composition and collection truck compartment design on GIS route optimization. *Waste Management*, *102*, 613-623.

Wang, H. F., & Chen, Y. Y. (2012). A genetic algorithm for the simultaneous delivery and pickup problems with time window. *Computers & Industrial Engineering*, *62*(1), 84-95.

Wang, J., & Rakha, H. A. (2018, November). Virginia Tech Comprehensive Powered-based Fuel Consumption Model: Modeling Compressed Natural Gas Buses. In *2018 21st International Conference on Intelligent Transportation Systems (ITSC)* (pp. 1882-1887). IEEE.

Wang, M., Miao, L., & Zhang, C. (2021). A branch-and-price algorithm for a green location routing problem with multi-type charging infrastructure. *Transportation Research Part E: Logistics and Transportation Review*, *156*, 102529.

Wei, Q., Guo, Z., Lau, H. C., & He, Z. (2019). An artificial bee colony-based hybrid approach for waste collection problem with midway disposal pattern. *Applied Soft Computing*, *76*, 629-637.

Xiang, Z., Chu, C., & Chen, H. (2006). A fast heuristic for solving a large-scale static dial-a-ride problem under complex constraints. *European Journal of Operational Research*, *174*(2), 1117-1139.

Xu, Y., Gbologah, F. E., Lee, D. Y., Liu, H., Rodgers, M. O., & Guensler, R. L. (2015). Assessment of alternative fuel and powertrain transit bus options using real-world operations data: Life-cycle fuel and emissions modeling. *Applied Energy*, *154*, 143-159.

Zbib, H., & Wøhlk, S. (2019). A comparison of the transport requirements of different curbside waste collection systems in Denmark. *Waste Management*, *87*, 21-32.

Zhang, S., Wu, Y., Liu, H., Huang, R., Yang, L., Li, Z., & Hao, J. (2014). Real-world fuel consumption and CO2 emissions of urban public buses in Beijing. *Applied Energy*, *113*, 1645-1655.

Appendix A

The parameters used in our CMEM are shown in Table A1.

Table A1
Parameters used in the HWCP model

Notation	Description	Value
g	Gravitational constant (meter/second^2)	9.81
ρ	Air density (kilogram/meter^3)	1.2041
A	Frontal surface area of the vehicle(meter^2)	3.912
C_r	Coefficient rolling friction	0.01
C_d	Coefficient of aerodynamic drag	0.7
w	Vehicle mass (kilogram)	6,350
v	Vehicle speed (km/h)	50
α_{ij}	Angle of the road slope between nodes i and j	Between -6% and 6%
∂^+	Energy efficiency in motor mode	0.76
∂^-	Energy efficiency in recuperating mode	1.27
c_e	Unit electric cost (dollar/kW)	0.11067
c_r	Unit CNG cost (dollar/liter)	0.98[a]
ξ	Fuel-to-air mass ratio	1
τ	Heating value of typical CNG fuel (kilojoules per gram)	38[b]
£	Engine friction factor (kilojoules per revolution per litter)	0.2

N	Engine speed (revolution per second)	33
D	Engine displacement(liters)	5
ϑ	Factor converting the fuel rate (grams per second to liters per second)	737
μ	Efficiency parameter for CNG engines	0.90
μ_t	Drive train efficiency	0.4
H^e	Capacity of battery (kW)	40
H^r	Capacity of CNG tank (GGE)	30

[a] *Estimated value from NGC (2017)*
[b] *Estimated value from Hagos et al.(2016)*